理學博士學位論文

패혈증 비브리오균에서 포도당 유무에 따른 HPr의 pyruvate kinase A 활성 조절

Regulation of pyruvate kinase A activity by HPr in response to glucose in *Vibrio vulnificus*

2015年 2月

서울大學校 大學院

生命科學部

金 惠 敏

패혈증 비브리오균에서 포도당 유무에 따른 HPr 의 pyruvate kinase A 활성 조절

指導敎授 石 暎 宰

이 論文을 理學博士學位論文으로 提出함

2014年 12月

서울大學校 大學院

生命科學部

金惠敏

金惠敏의 理學博士學位論文을 認准함

2014年 12月

委 員 長 노 정 혜

副委員長 서 영 재

委 員 이 기 로

委 員 최 상 호

委 員 최 희 정

Abstract

Regulation of pyruvate kinase A activity by HPr in response to glucose in *Vibrio vulnificus*

Hey-Min Kim

Department of Biological Sciences

The Graduate School

Seoul National University

The bacterial phosphoenolpyruvate:sugar phosphotransferase system (PTS) consists of two general proteins (enzyme I and histidine phosphocarrier protein) and several sugar-specific enzyme IIs (EIIs). In the case of the glucose PTS, EII consists of the cytoplasmic enzyme IIA^{Glc} ($EIIA^{Glc}$) and the membrane associated enzyme $IICB^{Glc}$ ($EIICB^{Glc}$). During the uptake of glucose, the phosphoryl group is transferred from phosphoenolpyruvate (PEP) to glucose in order of PEP

→ enzyme I (EI) → histidine phosphocarrier protein (HPr) → $EIIA^{Glc}$ → $EIICB^{Glc}$ → glucose. In addition to the phosphorylation-coupled transport of sugars, PTS proteins participate in various physiological processes through protein-protein interaction depending on their phosphorylation state.

Vibrio vulnificus is an opportunistic human pathogen that causes severe and often fatal infections in susceptible individuals. Although regulatory roles of the PTS have been extensively studied in *Escherichia coli*, much less is known about the *Vibrio vulnificus* PTS. To elucidate regulatory roles of the *V. vulnificus* PTS, ligand fishing was performed using HPr as bait. A HPr-binding protein in *V. vulnificus* was revealed as an ortholog of *E. coli* pyruvate kinase A (ePykA), and it was named a vPykA standing for *Vibrio* pyruvate kinase A. Pyruvate kinase (PK) catalyzes the final step of glycolysis, which is the transfer of a phosphoryl group from PEP to ADP, generating the products ATP and pyruvate for anaerobic and aerobic metabolism. The interaction between HPr and vPykA was strictly dependent on the presence of inorganic phosphate, and only dephosphorylated HPr interacted with vPykA. Experiments involving domain swapping between the PykAs of *V. vulnificus* and *E. coli* revealed the requirement for the C-terminal domain of vPykA for a

specific interaction with *V. vulnificus* HPr. Because the binding site for the allosteric effector is located at the C-terminal domain of PKs and the C-terminal domain determines the specificity of the HPr-vPykA interaction, the effect of HPr as an allosteric regulator of vPykA was assessed by a lactate dehydrogenase (LDH)-coupled enzyme assay. Only dephosphorylated HPr decreased the K_m of vPykA for PEP by approximately four-fold without affecting V_{max}.

To elucidate physiological roles of vPykA, the vPykA-deficient mutant (*pykA* mutant) was constructed. the *pykA* mutant cells entered the viable but nonculturable (VBNC) state much faster than wild-type cells when 5 x 10^6cells of each of the two strains were incubated in Luria-Bertani medium containing 2.5% NaCl (LBS) at 4℃. Several studies have provided evidence for the involvement of reactive oxygen species (ROS) in the VBNC state of *V. vulnificus* by showing that a significant portion of the VBNC population of *V. vulnificus* can be resuscitated if H_2O_2 scavenger (catalase or pyruvate) is present in the culture medium. Interestingly, a *pykA* mutant was more susceptible to H_2O_2 than wild-type *V. vulnificus*, and this sensitivity was completely rescued by the addition of pyruvate to the culture medium. Here, it is shown that *V. vulnificus* dephospho-HPr increases the affinity of vPykA for PEP to confer resistance to H_2O_2 stress in the presence of a

PTS sugar, such as glucose.

Keywords : H_2O_2 stress, phosphotransferase system, protein-protein interaction, regulation of glycolysis, *Vibrio vulnificus*

***Student Number* : 2010-30095**

CONTENTS

LIST OF FIGURES

LIST OF TABLES

ABBREVIATIONS

PTS, phosphoenolpyruvate:sugar phosphotransferase system

EI, enzyme I of the PTS

HPr, histidine phosphocarrier protein

Glc, glucose

PEP, phosphoenolpyruvate

PK, pyruvate kinase

LDH, lactate dehydrogenase

VBNC, viable but nonculturable

ROS, reactive oxygen species

FBP, fructose 1,6-bisphosphate

AMP, adenosine monophosphate

P_i, inorganic phosphate

MALDI-TOF, matrix-associated laser desorption ionization time-of-flight

SDS, sodium dodecyl sulfate

PAGE, polyacrylamide gel electrophoresis

SPR, surface plasmon resonance

CHAPTER I. Introduction

1. Epidemiology and pathogenesis of *Vibrio vulnificus*

1.1. Overview of *V. vulnificus*

Vibrio vulnificus is a motile, Gram-negative, curved rod-shaped bacterium with a single polar flagellum. It is distinguished from other members of the *Vibrio* genus in its ability to ferment lactose, and its presence in the estuarine environment is not due to pollution or other forms of contamination. Under certain conditions this bacterium has the ability to cause serious and often-fatal infections. Classically, the strains are grouped into 2 biotypes based on their physiological, biochemical, serological and host range differences (Amaro *et al.*, 1999). Biotype 1 is believed to compromise environmental and clinical isolates, and biotype 2 is thought to be an eel pathogen. This type differs from biotype one in other ways including the production of exoproteins and the O-antigenic side chain on the lipopolysaccharide molecule. A recently identified third biotype (biotype 3) appears to have emerged through the recombination of the genomes of biotypes 1 and 2 (Bisharat *et al.*, 1999).

V. vulnificus is a naturally occurring, free-living inhabitant of estuarine and marine environments throughout the world. It prefers tropical to subtropical climates, and has been isolated from waters where temperatures range from 9 to 31 ℃. It proliferates in areas or

during months where the water temperature exceeds 18 ℃ (Kaspar & Tamplin, 1993). Total viable *V. vulnificus* cells present in any location rises and falls with the ambient water temperature. At temperatures below 10 ℃, the number often drops to nearly undetectable levels. It is hypothesized that *V. vulnificus* survives by entry into a viable but nonculturable (VNBC) state in marine sediments (Oliver *et al.*, 1995). Laboratory experiments have shown that *V. vulnificus* enters the VNBC state at temperatures below 10 ℃ regardless of the nutrient level in the medium. There is a morphological change in the cells from rods to cocci, along with a change in membrane fatty acid profile, an increased mechanical resistance of the cell wall, and reduced amino acid transport. Resuscitation of the bacterium from the VNBC state is aided by a gradual increase in termperature in a nutrient-free medium (Oliver & Bockian, 1995), which may be analogous to the gradual warming of coastal waters in the spring.

1.2. Epidemiology of *V. vulnificus*

1.2.1. Types of infection and disease

V. vulnificus is an opportunistic human pathogen that causes serious and often fatal infections. These include an invasive septicemia usually contracted through the consumption of raw or undercooked shellfish, as

well as wound infections acquired through contact with shellfish or marine waters where the organism is present (Strom & Paranjpye, 2000). Primary septicemia is the most lethal infection caused by *V. vulnificus*, with an average mortality rate exceeding 50%. Symptoms include vomiting, diarrhea, abdominal pain, and a blistering dermatitis sometimes mistaken for pemphigus or pemphigoid. The majority of septic patients die of fulminant septicemia within 48 h after infection.

1.2.2. Host susceptibility

People who are most susceptible to *V. vulnificus* infection usually suffer from chronic disease that affects either liver function or the immune system (Tacket *et al.*, 1984). Liver disease includes cirrhosis or alcoholic liver disease, hepatitis or a history of hepatitis, metastatic cancer, or liver transplantation. Also included are hematological conditions that result in elevated serum iron levels including hemochromatosis and thalassemia major. Other conditions that predispose people to *V. vulnificus* infections include those with compromised immune systems (including chemotherapy and AIDS), other chronic diseases (diabetes mellitus, renal disease, chronic intestinal disease, or steroid dependency), or low gastric acid (therapeutically-induced or natural) (Shapiro *et al.*, 1998, Tacket *et al.*,

1984).

1.2.3. Clinical symptoms and treatment

The symptoms and severity of disease in people infected with *V. vulnificus* depends on the type of infection. Overall, the fatality rate for *V. vulnificus* ranges from 30–48% (Shapiro *et al.*, 1998); however, the fatality rate varies depending on the mode of infection and host factors. Patients with primary septicemia usually present with a sudden onset of fever and chills, often accompanied by vomiting, diarrhea, and abdominal pain as well as pain in the extremities. Within the first 24 h after onset of illness, secondary cutaneous lesions begin to appear on the extremities of many patients, including cellulitis, bullae, and ecchymosis. Up to 60% of patients suffer septicemic shock with systolic blood pressure less than 90 mm Hg. Within seven days, about half also exhibit mental status changes. In almost all cases of primary septicemia, *V. vulnificus* can be isolated from the blood and even the cutaneous lesions. Often these lesions become necrotic (necrotizing fasciitis) and require surgical debridement or amputation. Primary septicemia is fatal in 60–75% of patients; patients who become hyptotensive within 12 h of admission are more than two times likely to die compared with those with normal blood pressure (Klontz *et al.*,

1988). The symptoms suffered by patients with *V. vulnificus* wound infections are similar to those with primary septicemia, but differ in their timing and severity. Most patients report having an acute or preexisting wound in the week prior to onset of illness. There is inflammation at the wound site from which *V. vulnificus* can often be directly cultured. Wound infections can advance to cellulitis and become necrotic similar to that seen with primary septicemia. Often, these patients also become septicemic and suffer fever, chills, mental status changes, and hypotension. Rarely do cases of wound infections result in gastrointestinal symptoms. The fatality rate for *V. vulnificus* wound infections is lower than primary septicemia, ranging from 20–30%.

In cases of gastroenteritis that require hospitalization where *V. vulnificus* has been isolated from stool specimens, symptoms include fever, diarrhea, abdominal cramps, nausea, and vomiting. There is no systemic shock or localized cellulitis. As discussed earlier, the vast majority of *V. vulnificus*-associated gastroenteritis cases appear to be self-limiting, do not require hospitalization, and may largely go unreported.

Prompt antibiotic treatment of both systemic septicemia and wound infections is important for survival of the patient, as studies have shown

that the greater the delay between onset of illness and initiation of treatment, the higher the fatality rate. Tetracycline appears to be the most effective antibiotic for use in these infections, and has also been used in combination with gentamicin or chloramphenicol (Koenig *et al.*, 1991). Supportive care for shock and fluid loss is necessary, and in cases of cellulitis, aggressive surgical debridement and even amputation is often required. Similar to treatment regimens used in cases of *V. parahaemolyticus*-caused gastroenteritis, gastroenteritis attributed to *V. vulnificus* is managed by fluid replacement and, in severe cases, with antibiotic therapy.

1.3. Virulence factors of *V. vulnificus*

1.3.1. Polysaccharide capsule

V. vulnificus expresses an extracellular acidic polysaccharide capsule on its cell surface. Since the presence of capsular polysaccharide (CPS) is an important virulence determinant in many bacterial pathogens, the CPS of *V. vulnificus* has been extensively studied. Encapsulated isolates have an opaque colonial morphology but undergo a reversible phase variation to a translucent colony phenotype that is correlated with reduced or patchy expression of CPS (Wright *et al.*, 1990). The presence and amount of CPS on any given virulent isolate has been

positively correlated with quantitative measures of virulence of the organism in the mouse model. Translucent-phase variants are less virulent than opaque isolates, and strains with transposon mutations that result in loss of encapsulation have an LD_{50} more than four orders of magnitude higher than wild-type encapsulated strains.

1.3.2. LPS

LPS is a potent mediator of bacterial septic shock through the induction of host pyrogenic responses, and researchers have looked at the role of *V. vulnificus* LPS in the development of septic shock-like syndromes. In one study it was demonstrated that the LPS from *V. vulnificus* is less pyrogenic than LPS from other Gram-negative pathogens (McPherson *et al.*, 1991). Yet, a study by Espat et al. demonstrated that serum TNF-α levels paralleled the degree of *V. vulnificus* bacteremia in mice (Espat *et al.*, 1996). Although *V. vulnificus* CPS and LPS do not appear to be as pyrogenic as other enterobacterial endotoxins, they probably play an important role in modulation of the host cytokine response in vivo. They may have a synergistic effect on the host immune system by which they are important contributors in the induction of inflammation, tissue damage, and septicemic shock during systemic *V. vulnificus* infections.

1.3.3. Pili

Attachment and colonization of host surfaces are important steps in the early phase of infections of most bacterial infections. Often the initial attachment process is mediated by pili (also called fimbriae), which are proteinaceous fibers that protrude from the cell surface of many bacteria. Binding of pili to host cells is mediated by interactions between polypeptide domains on the pilus structure and specific host surface receptors (Strom & Lory, 1993). Only a few reports have described the presence of pili on *V. vulnificus*. In one study, Gander and LaRocco (Gander & LaRocco, 1989) described the presence of surface pili on a variety of *V. vulnificus* strains and reported that clinical isolates from blood or wounds of infected individuals averaged higher numbers of individual pilus fibers per cell than environmental isolates. In assays where they directly enumerated adherent bacteria on monolayers of HEp-2 cells, adherence correlated with increased piliation. Environmental isolates, on average, showed fewer bacteria adhering to individual epithelial cells.

1.3.4. Hemolysins

Two proteins with hemolytic activity have been described from *V.*

vulnificus. The most studied is the hemolysin termed ‘cytolysin’, a heat-labile, 56-kDa lytic enzyme that not only lyses mammalian erythrocytes, but also is extremely cytotoxic to a variety of tissue culture cell lines such as Chinese hamster ovary (CHO) cells (Gray & Kreger, 1985). In its purified form, this protein has been shown to cause vascular permeability in guinea pig skin and is lethal for mice, where it causes extensive extracellular edema and damage to capillary endothelial cells. The gene for the cytolysin has been cloned, sequenced and designated *vvhA*, and the encoded polypeptide shows 65% similarity in region I and 60% similarity in region II to the amino acid sequence of the *V. cholerae* El Tor hemolysin and the *V. cholerae* non-O1 cytolysin (Wright & Morris, 1991, Yamamoto *et al.*, 1990). It is secreted extracellulary via the type 2 pathway. However, its actual role in *V. vulnificus* infections is unclear because of the demonstration that there is no difference in the virulence of wild-type and isogenic strains unable to express the cytolysin. Interestingly, culture supernatant from a similar mutant constructed by insertion of an antibiotic resistance cassette in *vvhA*, is still cytotoxic for CHO cells. This suggests that *V. vulnificus* expresses other degradative enzyme(s) that have the potential to cause the rapid tissue destruction observed during *V. vulnificus* infections.

A second novel hemolysin was cloned and sequenced from a clinical *V. vulnificus* isolate (Chang *et al.*, 1997). The authors noted that in a screen of a number of *V. vulnificus* strains, most exhibited a clear hemolytic zone on agar medium containing rabbit erythrocytes but showed an ambiguous zone of green-brown color on sheep or human erythrocytes. Subsequent genomic cloning and screening for zones of hemolysis in *E. coli* carrying recombinant *V. vulnificus* DNA led to the isolation of several clones that did not contain *vvhA*, the cytolysin gene. Further analysis led to the characterization of an open reading frame, termed *vllY*, that encodes an approximately 40-kDa polypeptide. Expression of this gene in nonhemolytic *E. coli* results in zones of hemolysis and production of green color on human or sheep blood agar. The gene was shown to be present in all 41 *V. vulnificus* strains screened. The deduced amino acid sequence of VllY shows that it is related to legiolysin from *Legionella pneumophila*, a protein required for hemolysis, pigment production, and fluorescence. It is possible that the VllY hemolysin plays a role in the cytoxicity caused by culture supernatants from cytolysin (VvhA) nonexpressing strains. To date, there have been no further reports on the virulence of isogenic mutant strains unable to express VllY.

1.3.5. Metalloprotease

V. vulnificus produces an extracellular protease that possesses elastolytic and collagenolytic activities. This protease (designated VVP) is a metalloprotease requiring zinc for its catalytic activity (Miyoshi *et al.*, 1987). It is been suggested to be a potential virulence factor, particularly in skin lesions. In its purified form, it induces hemmorhagic damage, enhances vascular permeability and edema, is lethal in mice when administered i.p. or i.v., and subcutaneous injection causes rapid and extensive dermonecrosis. A recent study was undertaken to examine the phenotypic effects of a mutation in vvp. Lack of expression of the metalloprotease had no effect on the growth of the organism in vitro or in vivo, nor did it have an effect on induction of vascular permeablility in rats. Interestingly, there was an increase in the amount of cytolysin activity (as measured by hemolysis of mouse erythrocytes) in culture supernatants of the mutant compared to the isogenic wild-type strain. When examined for virulence in normal mice in an i.p. challenge, there was no difference in LD_{50} between wild-type and isogenic mutant strains. However, the LD_{50} of the metalloprotease-deficient mutant was reduced tenfold when force-fed to mice pretreated with cyclophosphomide (immunsuppressive) and iron dextran. The authors speculate that the cytolysin is a substrate of

the protease and that in the absence of the protease, more cytolysin is available to cause tissue damage, increasing virulence of the organism.

1.3.6. Iron

The importance of iron for growth of microorganisms has long been recognized, and because free iron is virtually absent in the human body, pathogenic bacteria have evolved mechanisms to scavenge iron from the iron transport proteins, transferrin and lactoferrin (Otto *et al.*, 1992). This is accomplished through the production of siderophores, many of which can acquire iron from transferrin or lactoferrin and subsequently deliver it to the bacterial cell. The role of iron and iron-acquisition systems seems particularly important for the virulence of *V. vulnificus* in light of the correlation between elevated serum iron levels, available free iron, and susceptibility to infection in both the mouse model and in humans. The inability to produce significant siderophores has been associated with reduced virulence, and it has been suggested that *V. vulnificus* may have the ability to obtain iron from transferrin and hemoglobin, with this ability correlated with virulence.

Shifting from a high- to a low-iron environment may also act as an important sensory signal to bacteria that they have entered a mammalian host. Many bacterial virulence determinants are regulated

by the iron status of a pathogen, with increased gene expression under low iron conditions (Litwin & Calderwood, 1993). One important factor in the transcriptional regulation by iron in many pathogens is the product of the fur gene. *V. vulnificus* was found to contain a fur homologue, which was shown to functionally complement a *V. cholerae* fur mutant. An isogenic *V. vulnificus* fur mutant constitutively expressed at least two iron-regulated proteins. The gene for one of these, a 77-kDa protein, was cloned and shown to have considerable homology to *V. cholerae* HupA, a heme receptor (Litwin & Byrne, 1998). A corresponding *V. vulnificus* hupA mutant was shown to lose the ability to use hemin or hemoglobin as a source of iron, and it is hoped that future studies with this mutant will help determine the role of heme iron in *V. vulnificus* pathogenesis.

1.4. Viable but non-culturable state in *V. vulnificus*

1.4.1. Characteristics of viable but non-culturable cells

Cultivation is one of the most fundamental steps in microbiology, and the plate count technique is one of the standard cultivation methods for the enumeration of viable bacteria. However, it was first discovered in 1982 that *Escherichia coli* and *Vibrio cholerae* cells could enter a distinct state called the viable but non-culturable (VBNC) state (Xu *et*

al., 1982). Unlike normal cells that are culturable on suitable media and develop into colonies, VBNC cells are living cells that have lost the ability to grow on routine media, on which they normally grow.

Despite their non-culturability on normally permissive media, VBNC cells are not regarded as dead cells because of various dissimilarities. Dead cells have a damaged membrane that is unable to retain chromosomic and plasmidic DNA, while VBNC cells have an intact membrane containing undamaged genetic information (Heidelberg *et al.*, 1997). The plasmids, if any, are also retained in VBNC cells (Oliver, 2010). While dead cells are metabolically inactive, VBNC cells are metabolically active and carry out respiration (Besnard *et al.*, 2002). Moreover, dead cells do not express genes, while VBNC cells continue transcription and therefore, mRNA production (Lleo *et al.*, 2000). In contrast to dead cells that no longer utilize nutrients, VBNC cells were shown to have continued uptake and incorporation of amino acids into proteins. Although VBNC cells have many general characteristics as a kind of viable cells, they have a lot of physiological and molecular differences from the viable, culturable cells. These differences include cellular morphology, cell wall and membrane composition, metabolism, gene expression, physical and chemical resistances, adhesion properties and virulence potential.

Ingeneral, VBNC cells have higher physical and chemical resistance than culturable cells, which might be due to their reduced metabolic rate and a cell wall strengthened by increased peptidoglycan cross-linking (Signoretto *et al.*, 2000). A recent study has shown that *V. vulnificus* in VBNC state has a higher resistance to a variety of challenges, including heat, low pH, ethanol, antibiotic, heavy metal, oxidative and osmotic stress, than those growing in exponential phase (Nowakowska & Oliver, 2013). VBNC cells can also show changes in adhesion and virulence properties. In *V. vulnificus*, the progressive reduction of virulence is time dependent (Oliver & Bockian, 1995).

1.4.2. The occurrence of VBNC cells and their importance

Many species of bacteria enter the VBNC state when they are exposed to stressful conditions such as starvation and low temperatures, suggesting that this is an adaptive strategy for long-term survival of bacteria under unfavorable environmental conditions (Ducret *et al.*, 2014). This hypothesis is supported by some characteristics of VBNC cells, including higher resistance to exogenous stresses, the ability of long-term survival under stress and the ability of resuscitation.

The ability to enter the VBNC state may be advantageous for bacteria, but poses a risk to human health. If VBNC cells are present,

the total number of viable bacteria in a sample will be underestimated by the CFU count method due to the inherent non-culturability of VBNC cells. Even worse, if all bacteria in the sample are in VBNC state, the sample may be regarded as germ-free due to non-detection. For bacterial species causing human infections, the underestimation or non-detection of viable cells in quality control samples from the food industry and water distribution systems, or clinical samples may pose serious risks to the public. The risks emerge from the fact that pathogenic bacteria can be avirulent in the VBNC state but regain virulence after resuscitation into culturable cells under suitable conditions (Du *et al.*, 2007). The identification of conditions that can induce bacteria to enter VBNC state and the underlying mechanisms, as well as the understanding of resuscitation conditions and mechanisms are necessary to effectively prevent bacterial infections and cure infected patients.

2. Phosphoenolpyruvate:sugar phosphotransferase system

2.1. Overview of phosphoenolpyruvate:sugar phosphotransferase system in *Escherichia coli*

Phosphoenolpyruvate:sugar phosphotransferase system (PTS) is ubiquitous in eubacteria but do not occur in eukaryotes. The bacterial

PTS plays an important role in the transport of numerous sugars, including glucose, mannose, fructose and cellobiose (Kundig *et al.*, 1964). The PTS is a member of group translocation. It is composed of two general cytoplasmic proteins, enzyme I (EI) and histidine phosphocarrier protein (HPr), which are used for all sugars, and a variable number of sugar-specific transport complexes collectively known as enzyme IIs (Postma *et al.*, 1993). EI transfers phosphoryl groups from phosphoenolpyruvate (PEP) to HPr. HPr then transfers the phosphoryl groups to the different enzymes II which together form a cascade of phosphorylated intermediates that transfer a phosphate from PEP to the incoming sugars. Carbohydrate phosphorylation is coupled to its translocation across the cytoplasmic membrane, and the energy for these processes is provided by the glycolytic intermediate PEP. PTS tranporters consist of three functional units, enzymes IIA, IIB and IIC. Enzymes IIA and IIB sequentially transfer phosphoryl groups from HPr to the transported sugars. Enzyme IIC contains the sugar binding site. EI, HPr and enzyme IIA are phosphorylated at His, while enzyme IIB domains are phosphorylated at either Cys or His depending on the particular transporter.

Proteins of the PTS also participate in numerous physiological processes in addition to their transport function. These proteins regulate

their targets either by protein-protein interaction or by phosphorylation. The regulatory roles of the PTS have been most extensively studied in *Escherichia coli*, and these roles include regulation of chemotaxis by EI (Lux *et al.*, 1995), regulation of glycogen phosphorylase and the anti-σ^{70} factor Rsd by HPr (Park *et al.*, 2013, Seok *et al.*, 2001, Seok *et al.*, 1997a), and regulation of the global repressor Mlc by the membrane-bound glucose transporter enzyme $IICB^{Glc}$ ($EIICB^{Glc}$) (Lee *et al.*, 2000, Nam *et al.*, 2001, Nam *et al.*, 2008, Tanaka *et al.*, 2000). In addition, enzyme IIA^{Glc} ($EIIA^{Glc}$) regulates carbohydrate transport and metabolism (Hurley *et al.*, 1993, Postma *et al.*, 1993, Seok *et al.*, 1997b), the metabolic flux between fermentation and respiration (Koo *et al.*, 2004), and adenylyl cyclase activity (Park *et al.*, 2006).

2.2. Components of glucose PTS in *E. coli*

The *ptsHIcrr* operon encodes the genes for the two common proteins of the PTS, EI and HPr, and the gene for $EIIA^{Glc}$. The proximity of the *crr* gene to those encoding the central PTS proteins appears to reflect the importance of these allosteric regulatory functions of $EIIA^{Glc}$ on carbon source utilization. The gene for $EIICB^{Glc}$, *ptsG*, is expressed as a single gene transcript. Both *ptsHIcrr* and *ptsG* operons are induced by growth on glucose.

E. coli EI, whose molecular weight is 63.5 kDa, is encoded by *ptsI* gene and phosphorylated by PEP at the N-3 position of His-189. The N-terminal domain of EI containing the His-189 active site, extends from residues 1 to 259 and can be phosphorylated in a fully reversible manner by phosphorylated HPr (Seok *et al.*, 1997a). The C-terminal domain is necessary for PEP binding and dimerization (Seok *et al.*, 1997b). Although EI and its N-terminal domain bind HPr with similar affinity, the C-terminal domain was shown to confer specificity with respect to interaction with various HPrs (Seok *et al.*, 1996). It has been known that autophosphorylation of EI requires of the dimeric form of the protein and requires divalent cations such as Mg^{2+} or Mn^{2+} (Chauvin *et al.*, 1994, Seok *et al.*, 1998).

E. coli HPr is a small, monomeric protein with a M_r, predicted from its amino acid sequence, of 9,119. Phosphoryl transfer from P-EI (His-189) to HPr is at the N1 position of His-15. HPr functions in transferring the phosphoryl group between EI and the various sugar specific enzyme IIs. Its size and heat stability have aided its purification from a variety of organisms. In addition, it is the first PTS protein whose three-dimensional structure has been studied by X-ray crystallography and solution multidimensional nuclear magnetic resonance (NMR) techniques.

E. coli EIIA^{Glc} is a protein with a M_r, predicted from its amino acid sequence, of 18,250. EIIA^{Glc} is phosphorylated by P-HPr at His-90 residue as an intermediate in PEP-dependent phosphotransfer to glucose (Dorschug *et al.*, 1984, Presper *et al.*, 1989). The N-terminus of EIIA^{Glc} appears to be important for its interaction with and phosphorylation of EIICB^{Glc} because proteolytic cleavage of the first 7 amino-terminal residues decreased the rate of phosphotransfer from EIIA^{Glc} to EIICB^{Glc} to 2-3% compared to intact EIIA^{Glc}. Site-directed mutagenesis studies coupled with the recent three-dimensional structure determination of EIIA^{Glc} from *E. coli* has provided clues to structure-function relationships in the phosphotransfer activity of this protein. As expected, replacement of the His-90 in EIIA^{Glc} from *E. coli* with Gln resulted in inactive protein that could not be phosphorylated by P-HPr. If the same substitution was made with the nearby His-75 in the *E. coli* protein, the mutant protein could still be phosphorylated by P-HPr but could not transfer the phosphate group to EIICB^{Glc} (Presper *et al.*, 1989). In *E. coli*, the level of phosphorylated EIIA^{Glc} reflects not only the availability of extracellular glucose but also the intracellular ratio of [PEP] to [pyruvate] (Hogema *et al.*, 1998).

The EIICB^{Glc} protein (50.7 kDa) consists of two domains, the N-terminal membrane-bound domain (EIIC; 41.1 kDa) which determines

the substrate specificity, and the C-terminal cytoplasmic domain (EIIB; 9.6 kDa) which is phosphorylated by $EIIA^{Glc}$ at Cys421. The system normally recognizes glucose as well as methyl-α-D-glucoside, 5-thio-D-glucoside, L-sorbose and, with a low affinity, mannose and 2-deoxyglucose (Garcia-Alles *et al.*, 2002). The phosphorylatable Cys421 on EIIB domain leads to artifactual disulfide crosslinking of subunits in the purified dimer. Next to Cys421, Arg424 and Arg426 are essential for glucose phosphorylation and transport, but not for the phosphorylation of $EIICB^{Glc}$ by $EIIA^{Glc}$. Only the C421S substitution abolishes phosphorylation of $EIICB^{Glc}$ by $EIIA^{Glc}$. The EIIC domain contains the sugar binding site, and point mutations conferring relaxed substrate specificity. It comprises eight putative membrane spanning segments, a topology which was first derived from the activity of fusion proteins between $EIICB^{Glc}$ and β-galactosidase or alkaline phosphatase and further confirmed by random linker insertion mutagenesis. A projection map of 2D crystals indicates a dimeric structure of $EIICB^{Glc}$, in agreement with results of inter-allelic complementation crosslinking and copurification of heterodimers (Siebold *et al.*, 2001).

2.3. PTS-mediated regulation in *E. coli*

2.3.1. Glucose PTS-mediated regulations

Important roles of the PTS include participation in a variety of physiological processes, including chemotaxis (Lux *et al.*, 1995), catabolite repression (Stulke & Hillen, 1999), carbohydrate transport and metabolism (Seok *et al.*, 1997b), carbon storage (Seok *et al.*, 1997a), and the coordination of carbon and nitrogen metabolism (Powell *et al.*, 1995). The regulatory functions of the PTS depend on the phosphorylation state of the involved component that increases in the absence and decreases in the presence of a PTS sugar substrate. The ratio of phosphorylated to dephosphorylated proteins in turn serves as signal input for the control of these physiological processes.

2.3.2. Carbon catabolite repression

Carbon catabolite repression (CCR) is the phenomenon in which the presence of carbon source metabolizable rapidly, like glucose, in the growth medium inhibits the gene expression and/or protein activity involved in the utilization of alternative carbon sources. If *E. coli* grows in a medium containing both glucose and lactose, it uses glucose preferentially until the sugar is exhausted. Then after a short lag, growth resumes with lactose as the carbon source. This biphasic growth pattern or response is called diauxic growth. The cause of diauxic

growth is not fully understood yet, but catabolite repression is known to play a major part. Prevention of the substrate-specific induction of catabolic genes has been identified as the major cause of preferential sugar utilization. By processes like inducer exclusion, inducer expulsion, or the control of the activity of regulators by phosphorylation, the PTS plays major roles during the process of CCR (Bruckner & Titgemeyer, 2002).

From the descriptions of major mechanisms of CCR it is apparent that the phosphorylation state of the PTS component, $EIIA^{Glc}$ determines regulatory responses in *E. coli*. Since $EIIA^{Glc}$/$P\text{-}EIIA^{Glc}$ is part of the regular PEP-PTS phosphoryl chain, defects in either of the two general PTS components will abolish CCR in *E. coli*. How the ratio of $P\text{-}EIIA^{Glc}$ to $EIIA^{Glc}$ could be adjusted according to sugar availability is immediately apparent considering PTS-mediated glucose transport. If glucose is transported, the phosphoryl group of $P\text{-}EIIA^{Glc}$ is delivered to incoming glucose via $EIICB^{Glc}$, so dephosphorylation of $EIIA^{Glc}$ would occur. Similarly, any PTS sugar could indirectly affect the phosphorylation state of $EIIA^{Glc}$ by draining phosphate groups to the incoming sugar.

Recently, the glycolytic pathway and its intermediates were implicated in additional regulatory events (Holtman *et al.*, 2001,

Kimata *et al.*, 2001). The dominant mechanism of glycerol kinase repression was found to be the allosteric inhibition by fructose 1,6-bisphosphate (FBP) rather than inhibition by $EIIA^{Glc}$. Blocking glycolysis resulted in a markedly reduced level of the main glucose transporter $EIICB^{Glc}$ caused by rapid decay of the $EIICB^{Glc}$ encoding *ptsG* mRNA. Hence, glycolysis and glycolytic intermediates could be more important for signal transduction in *E. coli* than anticipated.

2.3.3. Inducer exclusion

In *E. coli*, there is preferential transport and utilization of glucose via the PTS relative to sugars that are transported by other systems that are generally inducible. This phenomenon involves the phosphorylation state of the glucose-specific PTS protein $EIIA^{Glc}$. When a PTS sugar is transported, $EIIA^{Glc}$ becomes predominately unphosphorylated and allosterically inhibits several non-PTS permeases, including those for lactose (LacY), maltose (MalK), melibiose (MelB), and raffinose (RafB). This phenomenon is called inducer exclusion, since the preferred substrate or one of its metabolic derivatives inhibits entry of molecules that induce other metabolic systems. Dephospho-$EIIA^{Glc}$ also inhibits phosphorylation of glycerol by glycerol kinase, which catalyzes the first step in glycerol metabolism. Upon depletion of the

PTS sugar, $EIIA^{Glc}$ accumulates in the phospho-form, which relieves inducer exclusion and activates adenylate cyclase.

X-ray crystallography and NMR spectroscopy have elucidated the structures of both the phospho- and dephospho-forms of $EIIA^{Glc}$, showing that $EIIA^{Glc}$ undergoes only minor structural changes upon phosphorylation (Robillard & Broos, 1999). In addition, the X-ray structure of the $EIIA^{Glc}$- glycerol kinase complex and the NMR structure of the $EIIA^{Glc}$-HPr complex have been determined. A direct binding assay with $EIIA^{Glc}$ mutants was used to identify several residues in $EIIA^{Glc}$ that are important for binding to LacY. The $EIIA^{Glc}$ binding surface that interacts with glycerol kinase and HPr is similar and encompasses the $EIIA^{Glc}$ phosphorylation site along with the residues predicted to be important for binding to LacY.

2.3.4. Regulation of adenylate cyclase activity by $EIIA^{Glc}$

cAMP plays a central role in gene expression in enteric bacteria. Together with CRP, it is involved in the global regulation of a large number of catabolic genes. Mutants of enteric bacteria that lack any one constituent of the *pts* operon, EI, HPr or $EIIA^{Glc}$, normally exhibit very low rates of cAMP synthesis. These *in vivo* observations are attributed to a mechanism of adenylate cyclase regulation that involves

direct binding of and activation by phosphorylated $EIIA^{Glc}$ to the C-terminal domain of the adenylate cyclase protein (Peterkofsky *et al.*, 1993). $EIIA^{Glc}$ was proposed to relieve the inhibitory effect of this C-terminal domain on the N-terminal catalytic domain of adenylate cyclase (AC). Lately, it was demonstrated that a membrane-tethered form of AC (Tsr-AC) binds $EIIA^{Glc}$ specifically in vitro, regardless of its phosphorylation state and $EIIA^{Glc}$ binding is localized to the C-terminal region of AC (Park *et al.*, 2006). In the presence of an *Escherichia coli* extract, $P\text{-}EIIA^{Glc}$, but not $EIIA^{Glc}$, stimulates AC activity. These results allow for the formulation of a new model for the regulation of AC activity involving interaction of the regulatory domain of AC with both a regulatory factor and IIA^{Glc}, wherby the state of phosphorylation of IIA^{Glc} determines the level of AC activity.

2.3.5. Regulation of FrsA by $EIIA^{Glc}$

Koo *et al*. (2004) characterized a novel $EIIA^{Glc}$-binding protein from *E. coli* extracts, discovered using ligand-fishing with surface plasmon resonance spectroscopy. This protein, which named FrsA (*f*ermentation/*r*espiration *s*witch protein), is the 47-kDa product of the *yafA* gene, previously denoted as "function unknown." FrsA forms a 1:1 complex specifically with the unphosphorylated form of $EIIA^{Glc}$,

with the highest affinity of any protein thus far shown to interact with $EIIA^{Glc}$. Orthologs of FrsA have been found to exist only in facultative anaerobes belonging to the gamma-proteobacterial group. Disruption of *frsA* increased cellular respiration on several sugars including glucose, while increased FrsA expression resulted in an increased fermentation rate on these sugars with the concomitant accumulation of mixed-acid fermentation products. So, $EIIA^{Glc}$ regulates the flux between respiration and fermentation pathways by sensing the available sugar species via a phosphorylation state-dependent interaction with FrsA.

2.3.6. Interaction between acetate kinase and EI

Acetate kinase catalyzes the conversion of acetate and ATP into acetyl phosphate and phosphate. During the reaction, a phosphate group becomes linked to the enzyme via an acyl phosphate, a high-energy bond. In the presence of EI, HPr and $EIIA^{Glc}$ could be phosphorylated by ATP via acetate kinase (Fox *et al.*, 1986). P-EI can directly donate its phosphate group to acetate kinase, and the phosphate group of P-$EIIA^{Glc}$ can be transferred to acetate kinase in the presence of EI and HPr. Potentially, this reaction could form a link between the PTS and the enzymes connected to the Krebs cycle (Fox *et al.*, 1986). It remains to be demonstrated, however, that this alternative pathway for

phosphorylating PTS proteins in the absence of PEP is operative in an intact cell since this sequence of reactions has been shown only in an *in vitro* system.

2.3.7. Interaction between glycogen phosphorylase and HPr

Glycogen phosphorylase catalyzes the breakdown of glycogen into glucose-1-phosphate while the PTS affects the uptake of sugar substrates, like glucose, and hence both play a central role in carbohydrate metabolism. Seok *et al*. (1997a) found the direct interaction between HPr and glycogen phosphorylase using surface plasmon resonance spectroscopy. Although both HPr and P-HPr were shown to bind to glycogen phosphorylase, only dephosphorylated HPr stimulated the activity of glycogen phosphorylase. Moreover, it was shown that HPr regulates the intracellular concentration of glycogen *in vivo*, and thus, crosstalk between these two important carbon metabolic pathways is mediated by the phosphorylation state of HPr of the *E. coli* PTS. Furthermore, it was shown that the amount of unphosphorylated HPr but not that of glycogen phosphorylase is critical for the regulation of the intracellular glycogen level. Because the phosphocarrier function of HPr in the PTS allows the protein to exist in both phospho- and dephospho- forms, glycogen could be degraded in the presence of

glucose (Seok *et al.*, 2001).

2.3.8. Interaction between anti-σ^{70} factor Rsd and HPr

Promoter recognition and specific transcription initiation depend on the binding of a sigma factor to the core RNA polymerase in bacteria. The activity of sigma factors is often regulated through sequestration by cognate anti-sigma factors. Rsd, an anti-sigma factor known to complex with σ^{70} in stationary-phase cells, is known as a new HPr-binding protein in *E. coli*. Only the dephosphorylated form of HPr formed a tight complex with Rsd and, thus, inhibited complex formation between Rsd and σ^{70}. Dephosphorylated HPr, but not its phosphorylated form, antagonized the inhibitory effect of Rsd on σ^{70}-dependent transcriptions both *in vivo* and *in vitro* and also influenced the competition between σ^{70} and σ^{S} for core RNA polymerase in the presence of Rsd.

2.4. PTS in *V. vulnificus*

Simple sugars are present in the oceans in submicromolar concentrations, and they represent a significant fraction of the total available reduced carbon. Thus, marine bacteria must take up sugars by highly efficient transport systems, such as the PTS. The species that

compose the genus *Vibrio* are phenotypically diverse with respect to the utilization of certain sugars such as lactose and melibiose. The PTS occurred in all 15 species of *Vibrio* cross-reacted both immunologically and functionally with the corresponding proteins from the enteric bacteria such as *E. coli* and *S. typhimurium*. The members of the genus *Vibrio* possess a diverse array of phosphotransferase systems that are closely related to the systems in enteric bacteria but that also may differ in some important respects, particularly in the specificities of their sugar-specific receptor enzymes (Kubota *et al.*, 1979, Meadow *et al.*, 1987). The ubiquitous distribution of glucose and fructose and the *Vibrio* in the marine environment and the fact that the PTS appears to occur generally in the *Vibrio* leads to speculation that the PTS plays a critical role in regulation of the catabolism. In enteric bacteria, the PTS (primarily $EIIA^{Glc}$) regulates the catabolism of many non-PTS compounds. In *V. vulnificus*, the component proteins of the PTS are also highly conserved in enteric bacteria and crossreact with corresponding proteins with *E. coli*. And genetic organization of the PTS proteins in *V. vulnificus* is similar with that in *E. coli* which has *ptsHIcrr* operon encoding HPr, EI, $EIIA^{Glc}$ and separated ptsG gene encoding $EIIBC^{Glc}$ (Figure 1).

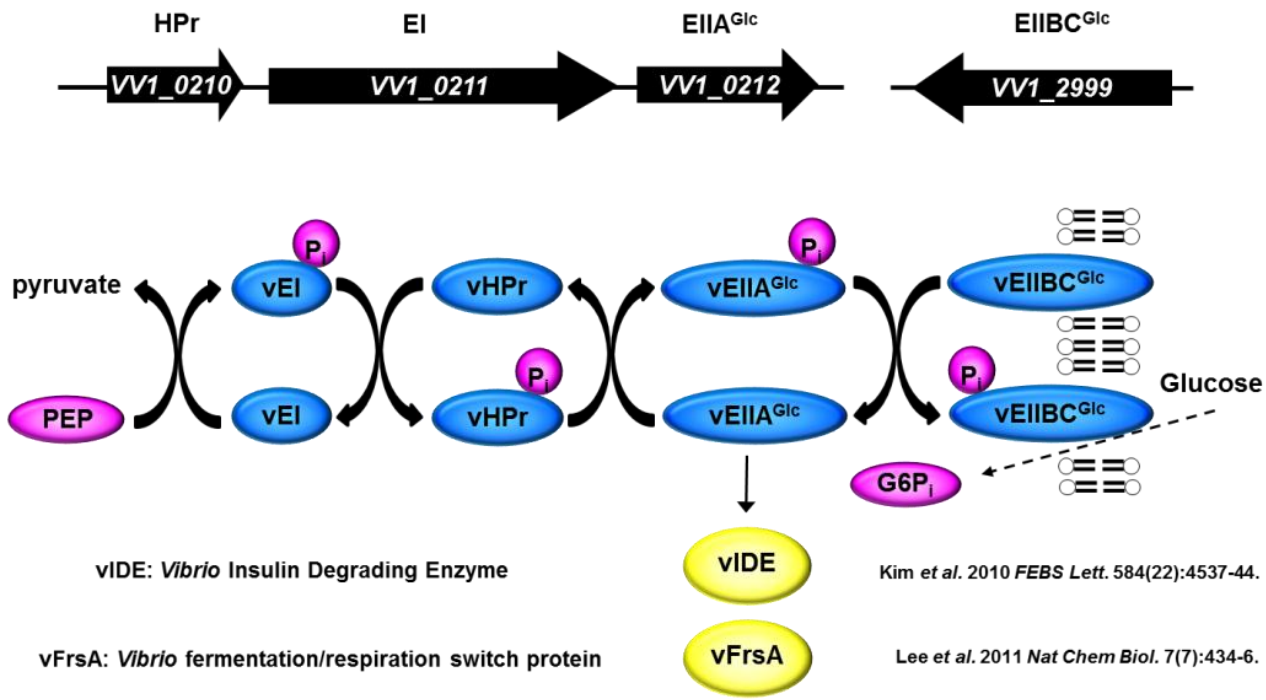
HPr
EI
EIIA^Glc
EIIBC^Glc
VV1_0210
VV1_0211
VV1_0212
VV1_2999
pyruvate
PEP
vEI
vEI
vHPr
vHPr
vEIIA^Glc
vEIIA^Glc
vEIIBC^Glc
vEIIBC^Glc
Glucose
G6P
vIDE
vFrsA
vIDE: Vibrio Insulin Degrading Enzyme
vFrsA: Vibrio fermentation/respiration switch protein
Kim et al. 2010 FEBS Lett. 584(22):4537-44.
Lee et al. 2011 Nat Chem Biol. 7(7):434-6.

Figure 1. Gene organization and roles of the glucose PTS in *V. vulnificus*.

In *V. vulnificus*, the component proteins of PTS are also highly conserved in enteric bacteria and crossreact with corresponding proteins with *E. coli*. And genetic organization of the PTS proteins in *V. vulnificus* is similar with that in *E. coli* which has *ptsHIcrr* operon encoding HPr, EI, IIA^{Glc} and separated *ptsG* gene encoding $IIBC^{Glc}$. In addition to the concomitant phosphorylation and translocation of glucose, the PTS takes part in a variety of physiological processes. For example, *V. vulnificus* enzyme IIA^{Glc} ($vEIIA^{Glc}$) interacts with and regulates the vIDE (which stands for Vibrio insulin-degrading enzyme) and vFrsA (Vibrio fermentation/respiration switch protein). The regulatory functions of the PTS depend on the phosphorylation state of the involved component, which increases in the absence and decreases in the presence of a PTS sugar substrate.

2.5. PTS-mediated regulation in *V. vulnificus*

2.5.1. Interaction between *Vibrio* insulin degrading enzyme (vIDE) and EIIA^{Glc}

Recently, the relationship between carbohydrate utilization and virulence has been studied in several human pathogenic bacteria such as *Listeria monocytogenes*, *Bacillus anthracis* and group A *Streptococcus* (Mertins *et al.*, 2007, Shelburne *et al.*, 2008, Tsvetanova *et al.*, 2007). In these species, the change of environmental carbohydrates acts as a signal to control their virulence gene expression through the regulation of a virulence transcription factor. Furthermore, glucose transport and metabolism via the carbohydrate PTS has been shown to be required for the successful infection of macrophages and mice by *Salmonella enterica* (Bowden *et al.*, 2009) and the colonization of mouse intestine by *Vibrio cholera* (Houot *et al.*, 2010).

In *V. vulnificus*, EIIA^{Glc} regulates the activity of a protease homologous to mammalian insulin-degrading enzymes by direct interaction. While specific interaction with the IDE homolog which is named as vIDE is independent of the phosphorylation state of EIIA^{Glc}, only unphosphorylated EIIA^{Glc} activates the peptidase activity of vIDE. Although the *ideV* (the gene encoding vIDE) mutant shows no growth defect *in vitro*, it shows significantly lower degrees of survival and

virulence than wild-type in mice (Kim *et al.*, 2010).

3. Pyruvate kinase in glycolytic pathway

3.1. Regulatory and functional properties of pyruvate kinase

Pyruvate kinase (PK), a final-stage enzyme in glycolysis, catalyzes the transfer of a phosphoryl group from PEP to adenosine diphosphate (ADP), generating the substrates ATP and pyruvate for anaerobic and aerobicmetabolism (Jurica *et al.*, 1998, Larsen *et al.*, 1994, Rigden *et al.*, 1999, Speranza *et al.*, 1989, Suzuki *et al.*, 2008, Valentini *et al.*, 2000). This reaction is essentially irreversible *in vivo* and appears to be one of the major control points for the regulation of the glycolytic flux. In addition, both substrate and products of this reaction feed into a number of energetic and biosynthetic pathways, placing PK at a primary metabolic intersection. The X-ray crystal structures of several PKs from different species (e.g., *Escherichia coli*, *Leishmania mexicana*, *Bacillus stearothermophilus*, cat, rabbit muscle, human erythrocyte, and yeast) revealed a high degree of structural homology in the general PK topology (Jurica *et al.*, 1998, Larsen *et al.*, 1994, Rigden *et al.*, 1999, Speranza *et al.*, 1989, Stuart *et al.*, 1979). PKs exist as homotetramers of identical subunits of ~50-60 kDa depending on species, each consisting of three to four domains: A, B, C,

and N-terminal domains. The N-terminal helical domain is absent in prokaryotic PKs and can be removed from human erythrocyte PK with no effect on its stability or activity (Valentini *et al.*, 2002). The A domain with β/α-barrel topology is located between the B (with β-barrel structure) and C (with α/β topology) domains. The active site lies at the interface of the A and B domains in each of the four subunits while the binding site for allosteric effector appears to be located at the C domain (Jurica *et al.*, 1998, Larsen *et al.*, 1994).

While there are four mammalian PK isozymes, M1, M2, L (liver), and R (red blood cell), with different primary structures, kinetic properties, and tissue distributions to satisfy the metabolic requirements of various tissues, most bacteria and lower eukaryotes have only one PK isoenzyme; only a few bacterial species (i.e., *E. coli* and *Salmonella typhimurium*) have two isoenzymes. PK is subject to various types of regulation, such as tissue-specific isozyme distribution, phosphorylation-dephosphorylation, and allosteric regulation, to regulate the switching between glycolysis and gluconeogenesis (Munoz & Ponce, 2003). Allosteric regulation, in particular, provides mechanisms for tight modulation of PK enzymes. All known PKs (except mammalian muscle M1 isoform) exhibit an inactive/active reversible association depending on allosteric activation by PEP and

one or more allosteric effector(s) whose precise chemical nature depends on the source of enzyme. Fructose 1,6-bisphosphate (FBP) acts as a potent allosteric activator of a number of PKs of different origin (e.g.,mammalian M2, L and R isozymes, yeast PK, and some bacterial PKs) (Dombrauckas *et al.*, 2005, Noguchi *et al.*, 1986, Valentini *et al.*, 2000), whereas in trypanosomatid protozoans *L. mexicana* and *Chlamydia trachomatis* the allosteric activator is fructose 2,6-diphosphate (F26BP) (Iliffe-Lee & McClarty, 2002, Rigden *et al.*, 1999, van Schaftingen *et al.*, 1985). The relationship of structure to this allosteric regulation of PK activity is not fully understood. However, it was shown recently that the transition between inactive T-state and active R-state involved a symmetrical 6˚ rigid-body rocking motion of the A- and C-domain cores in each of the four subunits. This also involved the formation of eight essential salt-bridge locks across the C-C interface that provided tetramer rigidity and a 7-fold increase in enzyme activity (Morgan *et al.*, 2010).

3.2. Characterization of bacterial pyruvate kinases

PKs have been isolated and characterized from numerous bacterial species (e.g., *E. coli* (Malcovati & Valentini, 1982), *B. stearothermophilus* (Sakai *et al.*, 1986), *Pseudomonas citronellolis*

(Chuang & Utter, 1979), *Streptococcus lactis* (Crow & Pritchard, 1982), *Lactobacillus bulgaricus* (Le Bras & Garel, 1993), *Mycobacterium smegmatis* (Kapoor & Venkitasubramanian, 1983), and *C. trachomatis* (Iliffe-Lee & McClarty, 2002). However, due to their general instability, bacterial enzymes have not been extensively studied. We know, nevertheless, that similar to eukaryotic PKs bacterial PKs demonstrate tight allosteric control by a variety of metabolite effectors.

The two most studied bacterial PK isoenzymes are those of *E. coli* (Ponce *et al.*, 1995, Waygood & Sanwal, 1974) and *Salmonella typhimurium* (D'Auria *et al.*, 2000), type I (PykF) and type II (PykA). Both enzymes show positive cooperative effects with respect to PEP; the type I enzyme is activated by fructose 1,6-bisphosphate (FBP) and type II by AMP (Garcia-Olalla & Garrido-Pertierra, 1987, Waygood *et al.*, 1976). The *E. coli* type II PK is also activated by several intermediates of the hexose phosphate pathway such as ribose 5-phosphate (Malcovati & Valentini, 1982). The *E. coli* type I and II PK isoenzymes just show a 33.1% identity between them and possess very different allosteric properties.

Genetic engineered microorganisms like *E. coli* in which PK genes have been inactivated or over expressed, exhibiting either native or alternative allosteric regulation, can increase the fluxes to a particular

metabolic product (Emmerling *et al.*, 1999, Ponce *et al.*, 1998).

4. Aims of this study

It has been known that PTS proteins regulate the function of many enzymes related to metabolic processes by direct interaction. While the proteins of the *E. coli* PTS have been shown to regulate numerous targets, there has been no direct evidence for the participation of two general PTS proteins (EI and HPr) in the regulation of other metabolic pathways in *V. vulnificus*. *V. vulnificus* HPr is a small, monomeric protein with an M_r of 9,094 predicted based on its deduced amino acid sequence. Given that HPr is known to be more abundant than $EIIA^{Glc}$ in enteric bacteria (Rohwer *et al.*, 2000), I assumed that there might be some regulatory mechanisms associated with *V. vulnificus* HPr. Ligand-fishing strategy was employed to discover the high affinity binding of HPr to a protein from *V. vulnificus* extracts. Physiological functions of *V. vulnificus* HPr could be inferred from the detected specific interaction and regulatory mechanism.

CHAPTER II. Materials and Methods

1. Construction of bacterial strains and plasmids

The bacterial strains and plasmids used in this study are listed in Table 1 and 2, respectively. All plasmids were constructed using standard PCR-based cloning techniques and verified by sequencing.

1.1. Deletion of vPykA gene

To construct a *pykA* deletion mutant of the *V. vulnificus* CMCP6 strain, a 1,079-bp DNA containing the *pykA* upstream region was amplified from the genomic DNA of *V. vulnificus* CMCP6 using two primers; 5′-GACCGTCTCGAGGCACCCTCTGTTGCCACAG -3′ (synthetic XhoI site underlined) and 5′- TGGCTGTCTAGAAGCTT CTCCTGCGATAGAC -3′ (synthetic XbaI site underlined). The PCR product was then cloned into the pDM4 vector (Milton et al., 1997 J Bacteriol) to produce pDM-PKAup. An 881-bp DNA fragment containing the downstream region of the *pykA* gene was amplified using the primers 5′- GTTTTTTCTAGACTCGCTTCATTAGTGATA G -3′ (synthetic XbaI site underlined) and 5′- AAAATTAGATCTTAT CCCTATAAGTTGGATC -3′ (synthetic BglII site underlined) and cloned into the corresponding sites of pDM-PKAup to result in pDM-ΔPKA. The *E. coli* SM10 λ*pir* strain carrying pDM-ΔPKA was conjugated with *V. vulnificus* CMCP6, and the transconjugants were

selected and integration was confirmed by PCR. To generate a *pykA* deletion mutant, the exoconjugants were then selected in LBS containing 8% sucrose (Lee *et al.*, 2011). Deletion of *pykA* in the selected colonies was confirmed by PCR.

1.2. Complementation of the *vpykA* mutant

To construct pRK-PKA, an 1,879-bp DNA fragment containing the *V. vulnificus pykA* gene and its own promoter was amplified using two primers, 5′- CATCTTGGATCC CAACATTCTATAACGGAGC -3′ (engineered BamHI site underlined) and 5′- CCAGTTCTGCAG TCAGCGGCCGAGACGAATTG -3′ (engineered PstI site underlined). The PCR product was cloned into the broad-host-range plasmid pRK415. The resultant plasmid, pRK-PKA, was transformed into *E. coli* SM10 λ*pir* and then transferred to the *pykA* mutant of *V. vulnificus* by conjugation.

1.3. Construction of chimeric PykA proteins

To construct pET-vePykA, a 998-bp DNA fragment containing the *V. vulnificus pykA* gene was amplified from the genomic DNA of *V. vulnificus* CMCP6 using two primers, 5′- AGGAGAACATATGACTC AGCCATTAAG AAG -3′ (engineered NdeI site underlined) and 5′-

ACTTCTGCCATGGAGCGCACCGTTTCGACTGG -3′ (engineered NcoI site underlined). The PCR product was then cloned into the pET3a vector to produce pET-vPykAup. A 446-bp DNA fragment containing the *E. coli pykA* gene was amplified from the genomic DNA of *E. coli* MG1655 using the primers 5′- TTGCAGCCATGG CGCGCGTTTGCCTGGGTGC -3′ (engineered NcoI site underlined) and 5′- CCGGCAGGATCCTTACTCTACCGTTAAAATACG -3′ (engineered BamHI site underlined) and cloned into the corresponding sites of pET-vPykAup to result in pET-vePykA.

To construct pET-evPykA, an 840-bp DNA fragment containing the *E. coli pykA* gene was amplified from the genomic DNA of *E. coli* MG1655 using two primers, 5′- AGTATTCCATGGGCTCCAGAAG GCTTCGCAGAAC -3′ (primer A, engineered NcoI site underlined) and 5′- GTGTTGCCGTGATTACCGCTCGGTTTAGCTGAC -3′. A 609-bp DNA fragment containing the *V. vulnificus pykA* gene was amplified from the genomic DNA of *V. vulnificus* CMCP6 using the primers 5′- CTAAACCGAGCGGTAATCACGGCAA CACAAATG -3′ and 5′- TAATGAGGATCCTTAGTCAAAAACAGGCAGG -3′ (primer B, engineered BamHI site underlined). The two PCR products were fused in a second round PCR using primers A and B, and the

obtained fragment was cloned into the NcoI and BamHI sites of pETDuet-1 to produce pET-evPykA.

Table 1. Bacterial strains used in this study.

Strains	Genotypes and/or descriptions	Source or reference
***V. vulnificus* strains**		
CMCP6	Clinical isolate	(Kim *et al.*, 2003)
CMCP6 *ΔpykA*		This study
CMCP6 *ΔpykF*		This study
***E. coli* strains**		
GI698	F^- λ^- *lac*I^q *lac*PL^8 ampC::P_{trp} cI	(LaVallie *et al.*, 1993)
GI698 *Δpts*	GI698 *Δ*(*ptsH, ptsI, crr*), Km^r	(Nosworthy *et al.*, 1998)
BL21 (DE3) pLysS	F^- l^- *ompT hsdS*$_B$(r_B^- m_B^-) *gal dcm met* (DE3) pLysS (Cm^R)	Novegen
SM10 λ*pir*	*thi-1 thr leu tonA lacY supE recA*::Rp4-2-Tc::Mu λ*pir*; Km^r	(Simon *et al.*, 1983)

Table 2. Plasmids used in this study.

Plasmids	Genotypes and/or descriptions	Source or reference
pRE-H-EI	pRE1-based expression vector for EI with N-terminal 6 His	(Kim *et al.*, 2010)
pRE-eHPr	pRE1-based expression vector for eHPr	(Seok *et al.*, 1997a)
pRE-H-eHPr	pRE1-based expression vector for eHPr with N-terminal 6 His	(Park *et al.*, 2013)
pET-vHPr	The ORF encoding vHPr was inserted into NdeI/XhoI sites of pET43.1a	This study
pET-H-vHPr	The ORF encoding vHPr with N-terminal 6 His was inserted into NdeI/XhoI sites of pET43.1a	This study
pET-vPykA	The ORF encoding vPykA was inserted into NcoI/BamHI sites of pET28a	This study
pET-H-vPykA	The ORF encoding vPykA was inserted into BamHI/PstI sites of	This study

	pETDuet-1	
pET-vPykF	The ORF encoding vPykF was inserted into NdeI/BamHI sites of pET3a	This study
pET-ePykA	The ORF encoding ePykA was inserted into NdeI/BamHI sites of pET3a	This study
pET-evPykA	See “Materials and Methods”	This study
pET-vePykA	See “Materials and Methods”	This study
pDM4	Suicide vector for homologous recombination into *V. vulnificus* chromosome, Cm^r	(Milton *et al.*, 1996)
pDM-PKAup	See “Materials and Methods”	This study
pDM-ΔPKA	See “Materials and Methods”	This study
pRK415	Broad host range vector, IncP *ori*, *oriT* of RK2; Tc^r	(Keen *et al.*, 1988)
pRK-vHPr	*V. vulnificus ptsH* promoter and ORF was cloned into BamHI/PstI sites of pRK415	This study
pRK-H15A	His15 of vHPr in pRK-vHPr was	This study

	mutated to Ala	
pRK-PKA	*V. vulnificus pykA* promoter and ORF was cloned into BamHI/PstI sites of pRK415	This study
pRK-PKA&H15A	*V. vulnificus ptsH* promoter and vHPr(His15Ala) was cloned into PstI/HindIII sites of pRK-PKA	This study
pBAD24	ColE1 *ori*; araBAD promoter; Ap^r	(Guzman *et al.*, 1995)
pJK1113	pKS1101 (pBAD24 with *oriT*) with *nptI*$^-$, Ap^r, Km^r	Laboratory collection
pJK-PKF	The ORF encoding vPykF was inserted into NcoI/SalI sites of pJK1113	This study

2. Media and cell culture

For the growth of GI698 and its derivative strains, M9 salts-based rich medium was used as described previously (Jeong *et al.*, 2004, LaVallie *et al.*, 1993, Seok *et al.*, 1997a) and these strains were cultured at 30 ℃. Other *E. coli* strains were cultured in Luria broth (LB) at 37 ℃. *V. vulnificus* strains were cultured in Luria-Bertani medium containing 2.5% NaCl (LBS) or M9 minimal medium containing 0.2% casamino acids and 2.5% NaCl (M9S). Usually *V. vulnificus* was cultured at 30 ℃.

3. Protein purification

Proteins with N-terminal His tags used in this study were overexpressed in the *E. coli* BL21 (DE3) strain, and purified using TALON metal affinity resin (Takara Bio, Japan) according to the manufacturer's instructions. The proteins were eluted with 200 mM imidazole and further purified by gel filtration chromatography using a HiLoad 16/60 Superdex 75 prep grade column (GE Healthcare) in 20 mM HEPES–NaOH (pH 7.6) containing 150 mM NaCl. Untagged proteins were overexpressed in *E. coli* BL21 (DE3) (vPykA, vPykF, ePykA, evPykA, vePykA, and vHPr) or the *E. coli* GI698*Δpts* strain (Nosworthy *et al.*, 1998) (eEI and eHPr). BL21 (DE3) cells were harvested 4 h after induction with 1 mM IPTG, and GI698 *Δpts* cells

were harvested 20 h after induction with 1 mM tryptophan. Cells were then disrupted by passing twice through a French pressure cell at 10,000 psi and were centrifuged at 100,000 *g* for 30 min at 4 ℃. The proteins in the supernatants were then purified using Mono Q 10/100 and HiLoad 16/60 Superdex 75 prep grade (GE Healthcare) column chromatography. Protein concentrations were determined with a bicinchoninic acid protein assay (Pierce) or Bradford assay (Bio-Rad).

4. Ligand fishing to search for proteins interacting with H-vHPr

4.1. Ligand fishing using protein bait

V. vulnificus CMCP6 cells grown at 30 ℃ overnight in LBS (100 ml) were harvested, washed and resuspended in 3 ml of buffer A (50 mM sodium phosphate, pH 7.0, containing 150 mM NaCl). Cells were disrupted by passing twice through a French pressure cell at 10,000 psi and then centrifuged at 100,000 *g* for 30 min at 4 ℃. The supernatant (1 ml) was mixed with 0.5 mg of His-tagged protein bait, and this mixture was incubated with 100 μl of TALON metal affinity resin at 4 ℃ for 30 min (Figure 2). After incubation, the resin was harvested and washed with 1 ml of buffer A three times, and the proteins bound to the resin were eluted with 100 μl of 2X SDS sample buffer. Aliquots

of the eluted protein samples were analyzed by SDS-PAGE and staining with Coomassie brilliant blue.

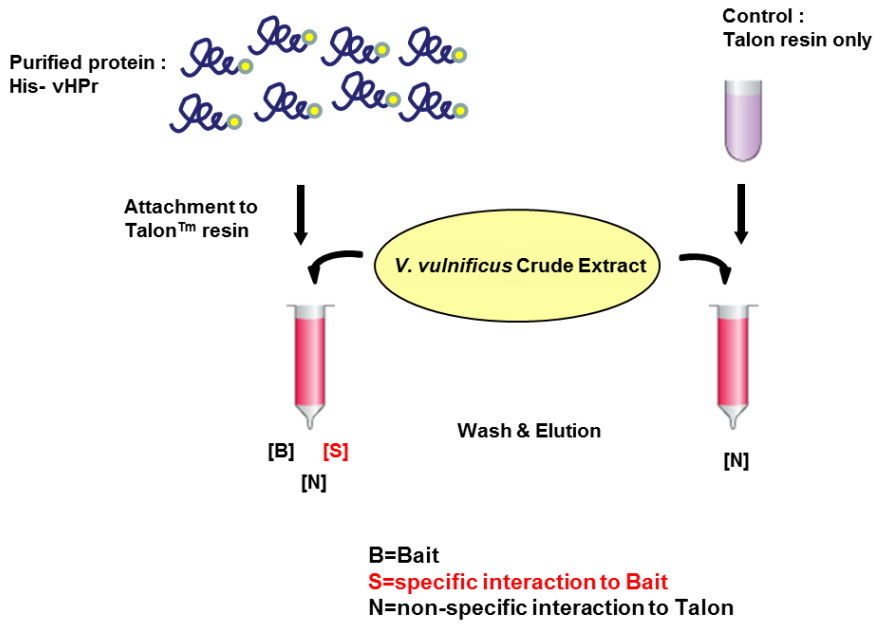

Figure 2. Schematic presentation of the fishing experiments.

Ligand fishing experiments were performed to search for a protein(s) that interacts with vHPr by using His-tagged vHPr (His-vHPr) as bait. His-vHPr was purified by BD Talon^{TM} metal affinity column and gel filtration. Cell lysate from *V. vulnificus* CMCP6 was mixed with or without His-vHPr in the columns, and the mixtures were subjected to pull-down assays by using a metal affinity resin. The proteins eluted specifically in a fraction containing His-vHPr were identified by in-gel digestion and MALDI-TOF analysis.

4.2. In gel-digestion

The polyacrylamide gel was stained with Coomassie Brilliant Blue R, and the bands of interest were excised from the gel. The gel fragments were washed with isopropyl alcohol and deionized water and equilibrated with 200 mM of ammonium bicarbonate for 20 min. The equilibrated gel fragments were dehydrated with 75% acetonitrile. Through this process, the gel fragments were destained. After the acetonitrile solutions were discarded and the gel fragments were dried in vacuum centrifuge. The polypeptides in the gel fragments were digested by the addition of trypsin at a concentration of 10 ng/μl and incubated overnight. The digested peptides were extracted three times with 20 μl of 75% acetonitrile containing 5% trifluoroacetic acid and concentrated to about 4 to 5 μl in a vacuum centrifuge. Mass spectra for peptide mapping of trypsin digests were acquired using a Voyager-DE^{TM} STR Biospectrometry Workstation (Applied Biosystems Inc.) matrix-assisted laser desorption ionization mass spectrometer.

5. RNA isolation and qRT-PCR

Total RNA was prepared using an RNeasy Mini kit (Qiagen) from *V. vulnificus* CMCP6 cells grown to logarithmic phase in LBS and M9S medium containing 0.2% glucose or galactose, and DNA was removed

using an RNase-free DNase (Promega). To determine the quantity of the gene of interest, a detection primer set was designed with Primer express® software 3.0 (Applied Biosystems Inc.). The same amount of RNA from each culture was converted into cDNA using cDNA EcoDry Premix (Clontech). cDNAs were diluted 20-fold and subjected to qRT-PCR analyses using gene-specific primers and SYBR Premix Ex Taq II (Takara). Amplification and detection of specific products were performed using the CFX96 Real-Time System (Bio-Rad). For normalization of the transcript level, the 16s rRNA gene was used as a reference. The relative expression level was calculated as the difference between the threshold cycle (C_t) of the target gene and the C_t of the reference gene for each template.

6. Surface plasmon resonance spectroscopy

The real-time interaction of vHPr with vPykA or vPykF was monitored by SPR detection using a BIAcore 3000 (BIAcore AB) as described previously (Lee *et al.*, 2007, Park *et al.*, 2013). Purified vHPr was immobilized on the carboxymethylated dextran surface of a CM5 sensor chip using a NHS/EDC reaction. The standard running buffer was 10 mM potassium phosphate (pH 7.5), 150 mM NaCl, 10 mM KCl, 1 mM $MgCl_2$, and 1 mM dithiothreitol (DTT), and all reagents were

introduced at a flow rate of 10 μl/min. The K_D value was determined using BIAevaluation 2.1 software.

7. Measurement of pyruvate kinase activity

Pyruvate kinase (PK) activity was determined by a continuous assay coupled to lactate dehydrogenase (LDH), in which the change in absorbance at 340 nm due to oxidation of NADH was measured using a spectrophotometer (Figure 3). The reaction contained 100 mM HEPES, pH 7.5, 200 mM KCl, 10 mM $MgCl_2$, 10 mM sodium phosphate, 1 mM DTT, 0.2 mM NADH, and 6 units of LDH (Sigma-Aldrich) in a total volume of 1 ml. Two millimolar ADP and 0-16 mM PEP were added as substrates to determine $S_{0.5}$ of vPykA for PEP in the presence or absence of 20 μM dephospho-HPr. Reactions were initiated by the addition of vPykA to a total concentration of 20 nM and continued at 30 °C for 5 min. PK activity was expressed as specific activity (μmol min^{-1} mg^{-1}), which is defined as the amount of PK that catalyzes the formation of 1 μmol of pyruvate/min. The apparent $S_{0.5}$, Hill coefficient (h), and V_{max} or k_{cat} values were determined by allosteric sigmoidal nonlinear regression analysis of data using the Prism software package (Graph Pad Inc., San Diego, CA).

Figure 3. Schematic view of the PK activity assay.

PK activity was determined by a lactate dehydrogenase (LDH)-coupled assay that measures the decrease in absorbance at 340 nm resulting from the oxidation of NADH to NAD^+.

8. Determination of the *in vivo* phosphorylation state of vHPr

Phosphohistidine residues are known to be very unstable at neutral and acidic pH, and 1-phosphohistidine residues, such as in phospho-HPr, are even less stable at pH <9.0 compared with the 3-phosphohistidine residues, such as in $EIIA^{Glc}$ (Hultquist, 1968); thus, exposure of samples to pH <9.0 was minimized. Furthermore, whereas $EIIA^{Glc}$ shows a phosphorylation-dependent mobility shift (PDMS) on SDS/PAGE, HPr shows a PDMS only on native PAGE (Lee *et al.*, 2013); therefore, to determine the *in vivo* phosphorylation state of vHPr, the procedure developed for $EIIA^{Glc}$ was modified significantly (Takahashi *et al.*, 1998). Cell cultures (0.5 ml at A_{600} = 1.0) were harvested and the supernatant fluids (0.3 ml) were discarded. The pellets were suspended in the rest supernatants (0.2 ml each) and disrupted at the same time by mixing with 60 μl of 5 M NaOH, followed by vortexing for 10 s and the addition of 100 μl of 3 M sodium acetate (pH 5.2) and 1 ml of 100% ethanol. The samples were centrifuged at 4 ℃ for at least 10 min. The pellet was suspended in 35 μl of native PAGE sample buffer containing 1 M urea, and 30 μl of this solution was immediately analyzed by 14% native PAGE. Proteins were then electrotransferred onto Immobilon-P (Millipore) following

the manufacturer's protocol and were detected by immunoblotting using antiserum against vHPr raised in rabbits. The protein bands were visualized using Immobilon Western chemiluminescent HRP substrate (Millipore) following the manufacturer's instructions.

9. Determination of the intracellular PEP and pyruvate concentrations

To determine the intracellular concentrations of PEP and pyruvate, 800 ml of cells were grown to $A_{600} = 1$, harvested by centrifugation, and washed with ice-cold M9S without a carbon source. Cells were diluted to a final volume of 2.6 ml with M9S, adjusted to room temperature for 5 min and aerated for 2 min before the indicated carbon source was added. Aeration was continued throughout the experiment. Samples (500 μl) were taken at the indicated times, mixed immediately with 250 μl of 5 M $HClO_4$, vortexed for 5 s and centrifuged at 5,000 *g* for 20 min at 4 ℃. Supernatants (500 μl) were neutralized with 170 μl of 5 M K_2CO_3. Precipitated $KClO_4$ was removed by centrifugation for 5 min in a chilled Eppendorf centrifuge. PEP and pyruvate were analyzed using spectrophotometry (Hogema *et al.*, 1998). The reaction mixture (total 1

ml) contained 200 μl of each sample plus 500 μl of reaction buffer containing 200 mM HEPES (pH7.5), 20 mM $MgCl_2$, 400 mM KCl, 2 mM DTT and 10 μl of freshly prepared 20 mM NADH. To measure pyruvate, the reaction was started by the addition of 1.5 units of LDH (Sigma-Aldrich). The A_{340} was observed after incubating at 30 ℃ for 20 min. Subsequently, for the determination of PEP, a PK (1 unit)/LDH (1.4 units) mixture (Sigma-Aldrich) was added with ADP (to 2 mM), and the A_{340} was observed after incubating at 30 ℃ for 20 min.

CHAPTER III. Results

1. Specific interaction between HPr and pyruvate kinase A in *Vibrio vulnificus*

1.1. Ligand fishing using *V. vulnificus* HPr as bait

To search for a protein(s) that interacts with *Vibrio vulnificus* HPr (hereafter vHPr), we used a ligand fishing strategy (Kim *et al.*, 2011, Kim *et al.*, 2010, Lee *et al.*, 2007, Park *et al.*, 2013). *V. vulnificus* CMCP6 crude extract was mixed with an N-terminally His_6-tagged form of vHPr (H-vHPr) and subjected to a pull-down assay. In several repeated experiments, we identified a protein band migrating with an apparent molecular mass of approximately 52 kDa that always co-eluted with H-vHPr (Figure 4). Peptide mapping of this protein band employing MALDI-TOF mass spectrometry analysis following in-gel digestion with trypsin indicated that the protein corresponded to a provisional pyruvate kinase encoded by *VV1_2992*.

Because pyruvate kinase (PK) catalyzes the final step of glycolysis, it is widespread in almost all types of organisms including animals, plants, fungi, and protists as well as bacteria. BLAST searches revealed that *V. vulnificus* strains have three genes encoding PK isozymes (*VV1_2992*, *VV1_0644*, and *VV2_0206*) like other vibrios. In contrast, *E. coli* strains have two PK isozymes: PykA (ePykA) is known to be allosterically activated by AMP, whereas PykF (ePykF) known to be allosterically

activated by fructose 1,6-bisphosphate. The PK encoded by *VV1_0644* shares 78 and 38% amino acid sequence identity with ePykF and ePykA of the *E. coli* K-12 strain, respectively, whereas the protein encoded by *VV1_2992* demonstrates 37 and 71% identity with ePykF and ePykA, respectively (Figure 5A). Although the PK encoded by *VV2_0206* shares a slightly higher sequence identity with ePykA (52%) than ePykF (40%), the presence of few mRNA transcripts of *VV2_0206* observed when the *V. vulnificus* CMCP6 strain was cultivated in different growth media suggests that *VV2_0206* expression may be cryptic (Figure 5B). Therefore, hereafter we refer to the PKs encoded by *VV1_0644* and *VV1_2992* as vPykF and vPykA, respectively.

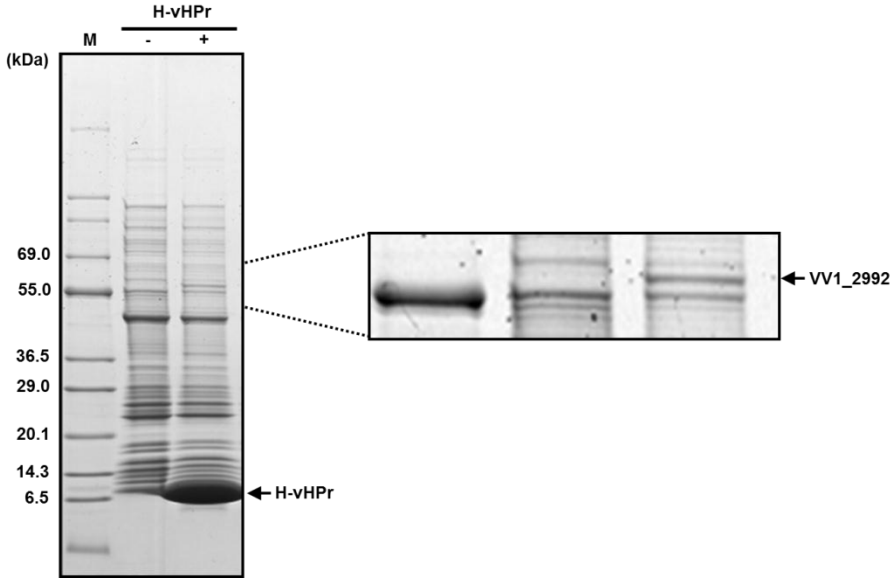
H-vHPr
M
-
+
(kDa)
69.0
55.0
36.5
29.0
20.1
14.3
6.5
H-vHPr
VV1_2992

Figure 4. Ligand fishing using His-tagged vHPr.

Ligand fishing experiment to search for protein(s) interacting with H-vHPr was carried out as described in the Materials and Methods. Crude extract prepared from *V. vulnificus* CMCP6 cells was mixed with TALON metal affinity resin in the presence (lane +) or absence (lane -) of purified His-tagged protein bait and subjected to metal affinity chromatography. After a brief wash, proteins bound to the resin were eluted, and the eluates were analyzed by SDS-PAGE using 4–20% gradient gels followed by staining with Coomassie brilliant blue. The protein bands that specifically bound to H-vHPr were excised from gels, and in-gel digestion and peptide mapping of tryptic digests were carried out as described previously (Jeong *et al.*, 2004). EzWay Protein Blue MW Marker (KOMA Biotech.) was used as the molecular mass marker (lane M).

A

% Identity	VV1_2992	VV1_0644	VV2_0206
ePykA	71	38	52
ePykF	37	78	40

B

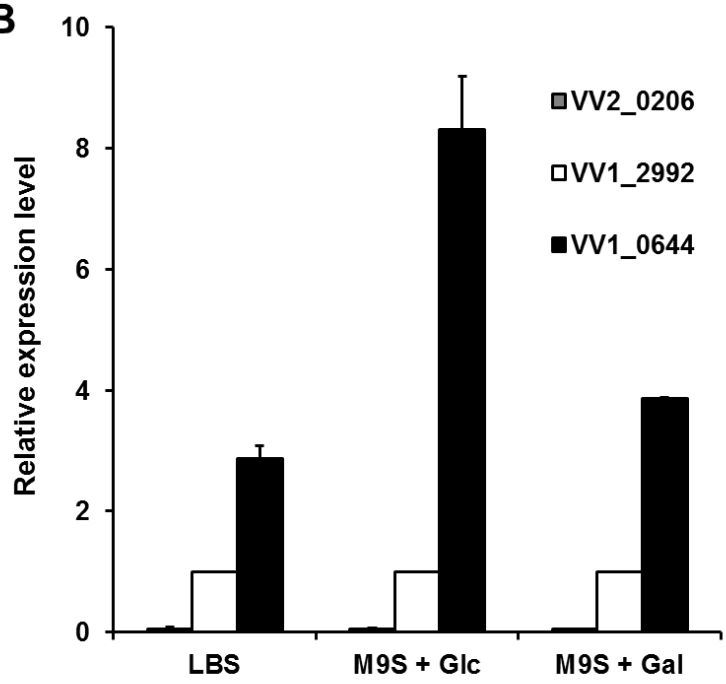

	LBS	M9S + Glc	M9S + Gal
VV2_0206	0.03 ± 0.02	0.01 ± 0.01	0.00 ± 0.01
VV1_2992	1.00	1.00	1.00
VV1_0644	2.87 ± 0.21	8.31 ± 0.88	3.87 ± 0.01

Figure 5. Comparison of pyruvate kinases in *V. vulnificus*.

A. Percent amino acid sequence identities between three pyruvate kinases (PKs) from *V. vulnificus* and two PKs from *E. coli*. Sequences were aligned using ClustalW software.

B. The relative transcript levels of the three PKs were determined by quantitative RT-PCR in wild-type *V. vulnificus* CMCP6 cells grown under different conditions as indicated. The results are presented as the relative levels (mean ± S.D. of triplicate determinations) compared to the transcript levels of VV1_2992.

1.2. Ligand fishing using vPykA as bait

To confirm the interaction between vPykA and vHPr, we constructed and purified His_6-tagged vPykA (H-vPykA). A pull-down assay was performed using TALON metal affinity resin charged with H-vPykA to identify vPykA-binding proteins from *V. vulnificus* CMCP6 crude extract. After a brief wash, proteins bound to the resin were eluted with 200 mM imidazole and analyzed by SDS-PAGE. As shown in Figure 6, a protein band migrating slightly slower than the 6.5 kDa polypeptide was detected only in the eluate from the column loaded with crude extract in the presence of H-vPykA. Peptide mass fingerprinting after in-gel tryptic digestion identified this protein as vHPr. This result supports a specific interaction between vHPr and vPykA.

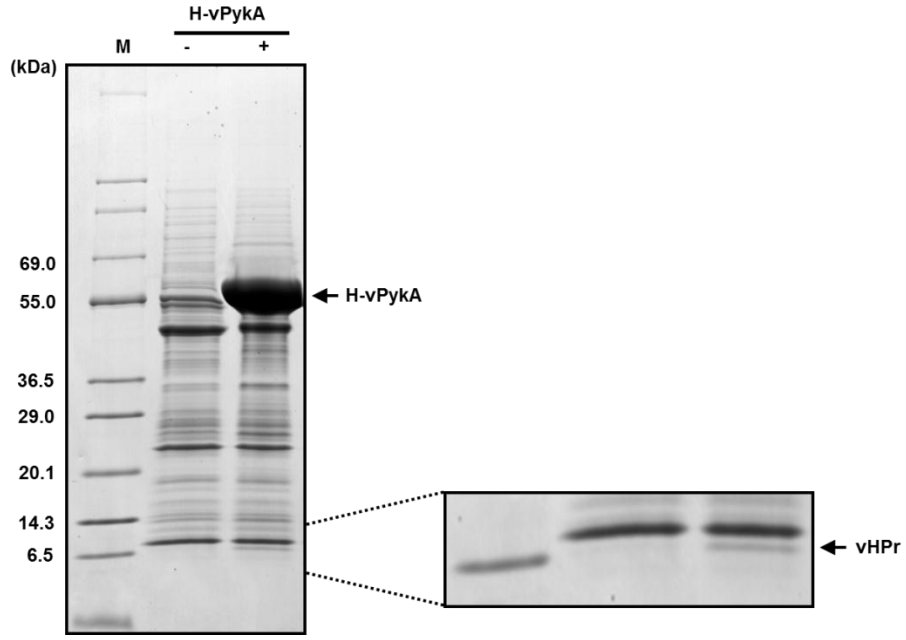

Figure 6. Ligand fishing using His-tagged vPykA.

Ligand fishing experiment to search for protein(s) interacting with H-vPykA was carried out as described in the Materials and Methods. Crude extract prepared from *V. vulnificus* CMCP6 cells was mixed with TALON metal affinity resin in the presence (lane +) or absence (lane -) of purified His-tagged protein bait and subjected to metal affinity chromatography. After a brief wash, proteins bound to the resin were eluted, and the eluates were analyzed by SDS-PAGE using 4–20% gradient gels followed by staining with Coomassie brilliant blue. EzWay Protein Blue MW Marker (KOMA Biotech.) was used as the molecular mass marker (lane M).

1.3. Dependence of the interaction between vHPr and vPykA on inorganic phosphate

To examine whether the interaction between vHPr and vPykA requires any additional factor(s), purified vPykA was mixed with purified H-vHPr and subjected to metal affinity chromatography. Unlike vPykA in crude cell extracts, the purified protein alone exhibited little binding to H-vHPr unless crude cell extract was added (Figure 7, lanes 1-3), implying that the interaction between vHPr and vPykA depends on an additional factor(s). To test whether this additional factor is a protein or a small metabolite, the crude cell extract was filtered using a Microsep 3K membrane, and the effect of the filtrate on the interaction was measured. Because vPykA exhibited binding to H-vHPr in the presence of the filtrate, we assumed that the factor required for the vPykA-vHPr interaction could be a small molecule (Figure 7, lane 4). Therefore, we tested the effects of various cellular metabolites on this interaction. While potassium glutamate, potassium acetate, and acetyl phosphate had little effect on vHPr-vPykA binding, potassium phosphate remarkably increased the binding of vPykA to vHPr (Figure 7, lanes 5-8), indicating that inorganic phosphate (P_i) is the mediator of the vHPr-vPykA interaction. It should be noted that 50 mM sodium phosphate

buffer was used in the initial fishing experiment to search for a new binding partner of vHPr (Figure 4).

Intracellular concentrations of P_i have been reported in the range of 3 to 9 mM for *E. coli* grown under normal conditions in the pioneering *in vivo* ^{31}P-NMR studies (Ugurbil *et al.*, 1982), although internal P_i can rise to higher levels when glycerol-3- phosphate is added to the medium (Xavier *et al.*, 1995). Therefore, we tested the effect of P_i concentration on the interaction between vHPr and vPykA. Consistent with the data in Figure 7, vPykA showed little specific binding to H-vHPr in the absence of P_i (Figure 8A, lane 1 and 2). However, as the concentration of P_i in the reaction mixtures was raised, the specific binding of vPykA to H-vHPr increased as well (Figure 8A and B). A double reciprocal plot revealed that the P_i concentration for half-maximal stimulation of the vPykA-vHPr interaction was approximately 3.95 mM (Figure 8C). Considering this result and the intracellular concentrations of P_i reported in *E. coli* (Ugurbil *et al.*, 1982), P_i was added to a final concentration of 10 mM, resulting in approximately 70% maximum stimulation, in all experiments hereafter unless otherwise specifically mentioned.

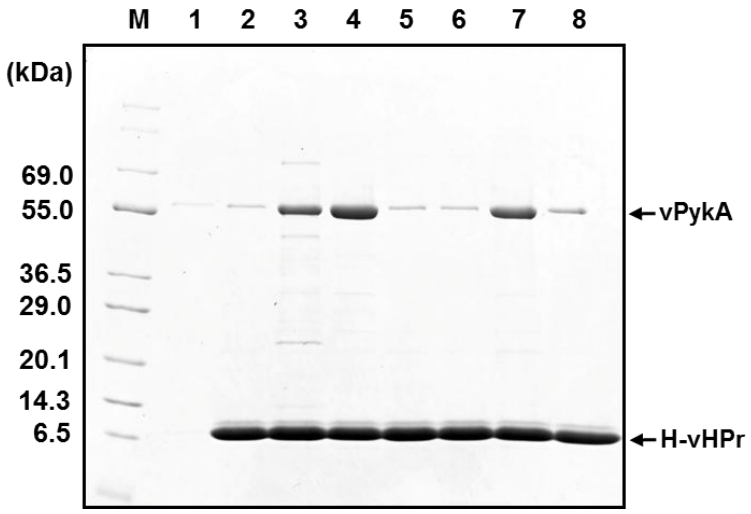
M 1 2 3 4 5 6 7 8
(kDa)
69.0
55.0
36.5
29.0
20.1
14.3
6.5
vPykA
H-vHPr

Figure 7. The interaction between vPykA and vHPr depends on inorganic phosphate.

The effect of various compounds on the interaction of vPykA with vHPr. Purified vPykA (100 μg) was mixed with purified H-vHPr (60 μg) in 20 mM HEPES–NaOH (pH 7.6) containing 150 mM NaCl in the presence or absence of various compounds and subjected to TALON metal affinity chromatography. The results were analyzed by 4–20% gradient SDS-PAGE and staining with Coomassie brilliant blue. Lane M, molecular mass markers (Koma Biotech, Inc.); lane 1, vPykA was added alone as control; lane 2, vPykA and H-vHPr; lane 3, vPykA, H-vHPr, and 50 μl of *V. vulnificus* crude extract used in Figure 4; lane 4, vPykA, H-vHPr, 50 μl of 3-kDa filtrate of *V. vulnificus* crude extract; lane 5, vPykA, H-vHPr, and potassium glutamate (to 10 mM); lane 6, vPykA, H-vHPr, potassium acetate (to 10 mM); lane 7, vPykA, H-vHPr, potassium phosphate (to 10 mM); lane 8, vPykA, H-vHPr, and acetyl phosphate (to 10 mM).

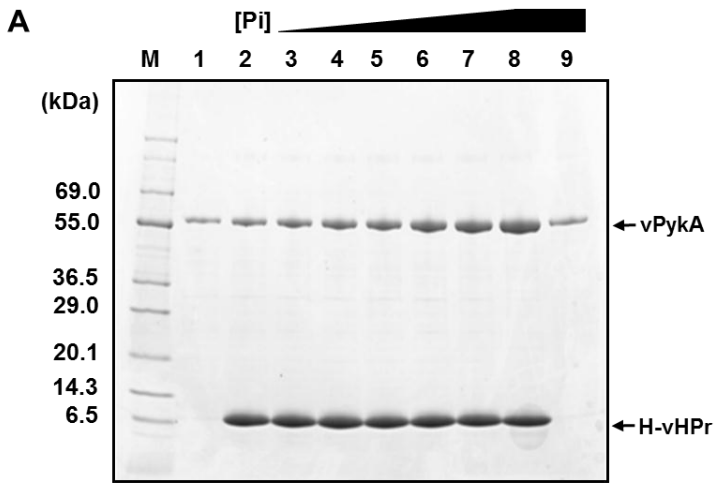
A
[Pi]
M 1 2 3 4 5 6 7 8 9
(kDa)
69.0
55.0
36.5
29.0
20.1
14.3
6.5
vPykA
H-vHPr

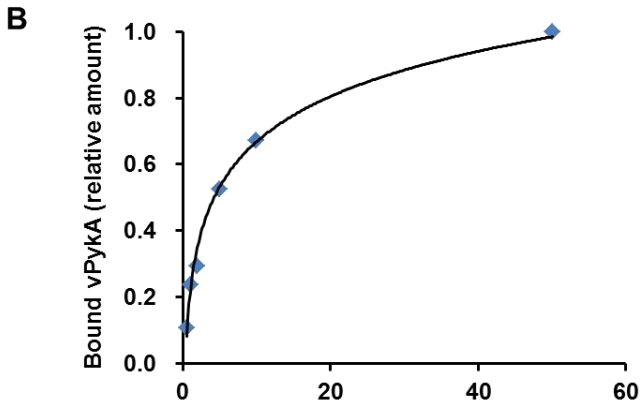
B
Bound vPykA (relative amount)
1.0
0.8
0.6
0.4
0.2
0.0
0
20
40
60

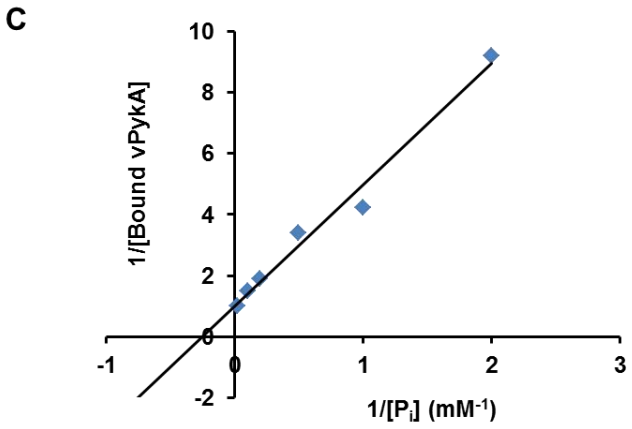
C
1/[Bound vPykA]
10
8
6
4
2
0
-2
-1
0
1
2
3
1/[Pi] (mM-1)

Figure 8. Inorganic phosphate-dependent interaction of vPykA to vHPr.

A. Effect of varying concentrations of sodium phosphate (P_i) on the interaction of vPykA with vHPr. vPykA (100 μg) and H-vHPr (60 μg) in 20 mM HEPES–NaOH (pH 7.6) containing 150 mM NaCl were incubated with increasing amounts of P_i (0, 0.5, 1, 2, 5, 10 and 50 mM; lanes 2-8) and subjected to pull-down assays. In lane 1 and 9, vPykA alone was incubated with 0 and 50 mM P_i, respectively, and subjected to pull-down assays as a loading control.

B. Plot of the P_i concentration-dependent binding of vPykA to H-vHPr. The Coomassie blue-stained gel in (A) was scanned, and the band intensities of vPykA were measured with the Multi Gauge program. The relative amounts of vPykA bound to H-vHPr were calculated based on the specific binding by subtracting the amount of vPykA bound to H-vHPr in 0 mM P_i from that bound to H-vHPr in each concentration of P_i as indicated.

C. Double reciprocal plot of 1/[Bound vPykA] *versus* 1/[P_i] using the data in (B).

1.4. Confirmation of the interaction between vHPr and vPykA by surface plasmon resonance (SPR)

The specificity of the interaction between vHPr and vPykA was determined by employing surface plasmon resonance (SPR) biosensor technology with the BIAcore system (Seok *et al.*, 1997a). vHPr was immobilized on a CM5 sensor chip, and vPykA or vPykF was allowed to flow over the surface. When purified vPykF was exposed to immobilized vHPr, no interaction was detected (Figure 9A, sensorgram **a**). In contrast, purified vPykA resulted in a significant increase in the SPR response (Figure 9A, sensorgram **b**), indicating that vHPr interacts with vPykA but not with vPykF. To determine kinetic parameters for the binding of vHPr to vPykA, different concentrations (31.25 - 500 μM) of purified vPykA were applied to the vHPr surface of the sensor chip. The signal increased as a function of vPykA concentration (Figure 9B). The dissociation constant (K_D) for the vHPr-vPykA interaction was determined using BIAevaluation software to be approximately 4.5 x 10^{-7} M, assuming a 1:1 interaction.

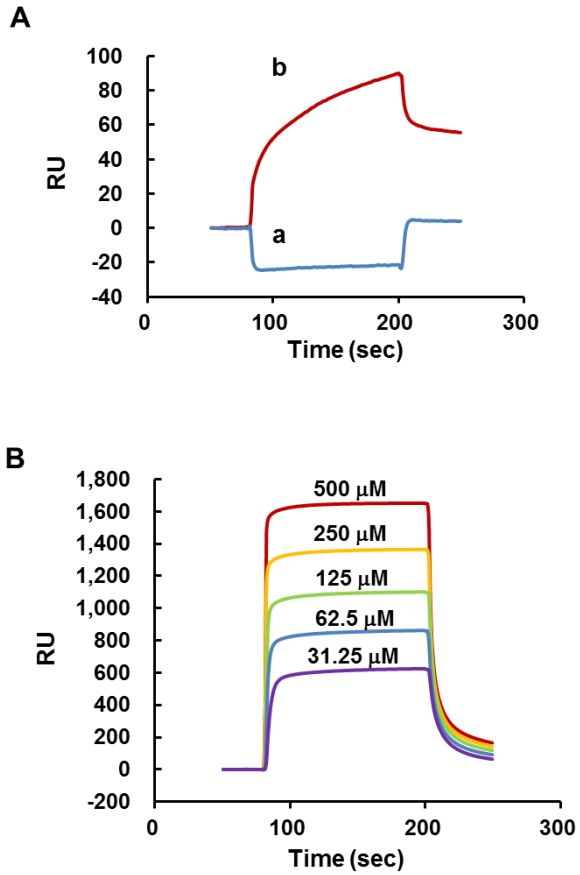

Figure 9. Analysis of the interaction between vHPr and vPykA by surface plasmon resonance (SPR).

A. vPykA (sensorgram **a**) or vPykF (sensorgram **b**) was allowed to flow over the vHPr surface.

B. Measurement of the dissociation constant (K_D) between vPykA and vHPr. The indicated amounts of vPykA were allowed to flow over the vHPr surface. The K_D value for the interaction between vHPr and vPykA was determined to be ~ 4.484×10^{-7} M.

1.5. Phosphorylation state-dependent interaction between vHPr and vPykA

Generally, the regulatory functions of the PTS depend on the phosphorylation state of the involved protein (Deutscher *et al.*, 2006). Accordingly, the effect of phosphorylation of vHPr on its interaction with vPykA was assessed by SPR. The phosphorylated and dephosphorylated vHPr surfaces were generated by reversible phosphoryl transfer reactions between EI, vHPr and $EIIA^{Glc}$ (Nam *et al.*, 2001). When purified vPykA was applied to immobilized vHPr, a high affinity interaction was detected (Figure 10, sensorgram **a**). In contrast, after immobilized vHPr was phosphorylated by allowing the mixture of EI and phosphoenolpyruvate (PEP) to flow over the surface and was subsequently washed with running buffer, an interaction with vPykA was barely detectable (Figure 10, sensorgram **b**). Furthermore, the same vHPr surface demonstrated recovered vPykA binding activity after dephosphorylation by flowing dephosphorylated $EIIA^{Glc}$ through the flow cell and flushing with running buffer (Figure 10, sensorgram **c**). These results indicate that only dephospho-vHPr, but not its phosphor-form, can interact with vPykA.

Specificity and dependence on phosphorylation state for the interaction between vHPr and vPykA was also examined via pull-down

assays with H-vHPr adsorbed to TALON metal affinity resin. The phosphorylated form of vHPr was generated by adding EI and PEP to the reaction mixtures. As expected for enzymes requiring divalent cations as cofactors (Muirhead, 1990), some nonspecific binding of both vPykA and vPykF to TALON metal affinity resin was observed. When a fixed amount of purified vPykA was mixed with different concentrations of dephosphorylated H-vHPr, the amount of vPykA pulled down by H-vHPr increased as the concentration of H-vHPr increased (Figure 11A). In contrast, when H-vHPr was phosphorylated by incubating with EI and PEP, the amount of vPykA bound to the resin was not affected by the concentration of vHPr added to the reaction mixture. As expected from the data in Figure 9A, H-vHPr adsorbed to TALON metal affinity resin did not pull down vPykF regardless of the phosphorylation state of vHPr (Figure 11B). These results support the specificity and dependence on the phosphorylation state of the vHPr-vPykA interaction.

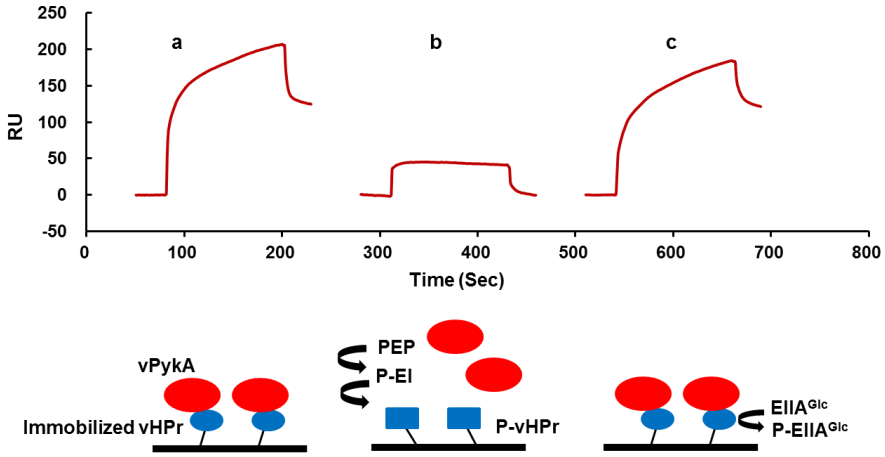

Figure 10. Phosphorylation state-dependent interaction between vPykA and vHPr by SPR.

Sensorgram **a** shows vPykA binding to the immobilized vHPr surface. In sensorgram **b**, vPykA was injected after the immobilized vHPr surface had been phosphorylated by exposing it to a mixture of EI and phosphoenolpyruvate (PEP), then flushing with running buffer to remove PEP and EI. In sensorgram **c**, dephosphorylated $EIIA^{Glc}$ was allowed to flow over the phosphorylated vHPr surface generated in sensorgram **b** to dephosphorylate the surface before vPykA was injected.

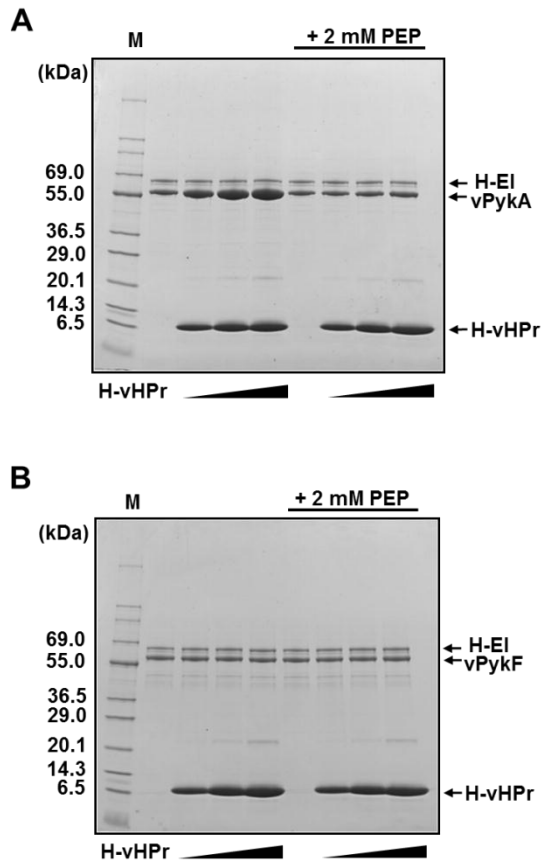

Figure 11. Phosphorylation state-dependent interaction of vPykA with vHPr.

Purified vPykA (A) or vPykF (B) (100 μg each) was incubated with 5 μg of H-EI and varying amounts of purified H-vHPr (0, 25, 50, and 100 μg) in the presence or absence of 2 mM PEP, and then mixed with 50 μl of TALON metal affinity resin. After incubation for 10 min, resin-bound proteins were eluted, resolved in SDS-PAGE gels, and stained with Coomassie brilliant blue.

1.6. The C-terminal domain of vPykA determines the binding specificity of the vHPr-vPykA complex

In a recent screen of proteins interacting with HPr employing a ligand fishing strategy in *E. coli*, we identified the anti-σ^{70} factor Rsd as a new target regulated by HPr (Park *et al.*, 2013). Whereas Rsd and glycogen phosphorylase, which has already been found to interact with HPr, were pulled down by HPr, we could not detect any interaction between HPr and PKs in *E. coli*. However, because BLAST searches revealed that vPykA and vHPr share 71 and 76% amino acid sequence identity with ePykA and *E. coli* HPr (hereafter eHPr), respectively, we assumed that the interaction of PykA with HPr might also occur in *E. coli*. To test whether the interaction between HPr and PykA is specific in *V. vulnificus* or whether cross-interactions are possible between proteins from other species, we prepared the HPr and PK proteins from *E. coli* and *V. vulnificus*, and measured the cross-interactivities of these proteins. Notably, neither vHPr nor eHPr interacted with vPykF and ePykA, while vPykA did interact with eHPr, albeit with lower affinity than with vHPr (Figure 12). These data indicate that the interaction between the HPr and PykA proteins is species-specific and dependent on the surface structure of PykA.

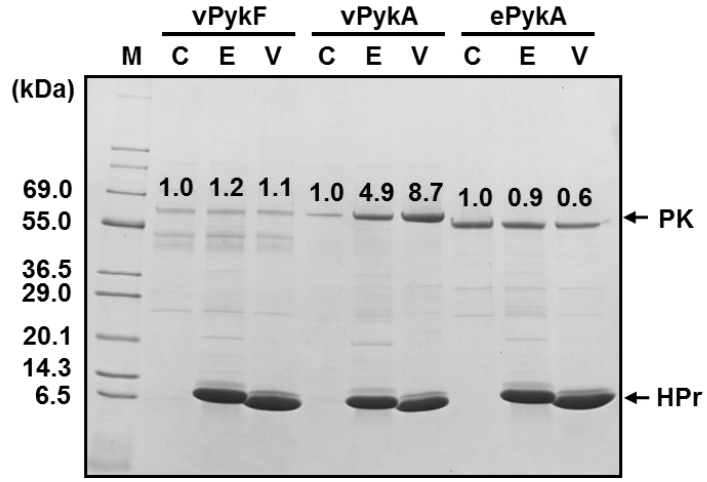

Figure 12. Test for the interaction between PKs and HPr proteins.

Purified vPykF, vPykA, and ePykA (60 μg each) were mixed with buffer control (lanes C), 100 μg of H-eHPr (lanes E) or H-vHPr (lanes V) in the presence of 50 μl of TALON resin. After metal affinity chromatography, proteins bound to each column were analyzed by 4–20% gradient SDS-PAGE and staining with Coomassie brilliant blue. Numbers above the PK bands represent the levels of PKs bound to HPr proteins relative to the level in lane C for each PK measured with Multi Gauge software. Lane M, molecular mass markers (Koma Biotech, Inc.).

PKs are highly conserved in all organisms from prokaryotes to eukaryotes. The generation of crystal structures for several PKs from various species of bacteria, yeast and mammals has revealed a generally conserved architecture (Mattevi *et al.*, 1995, Rigden *et al.*, 1999, Valentini *et al.*, 2002, Zoraghi *et al.*, 2011). PKs exist as homo-tetramers and each subunit consists of three or four domains: the N, A, B, and C domains. The N domain is not present in prokaryotic PKs, and the A and B domains at N-termini of these bacterial enzymes comprise 70%, where binding sites for ADP, PEP, and divalent cations are located. The remaining 30% corresponds to the C domain, where the binding site for the allosteric regulator is located. Alignment of the amino acid sequences of ePykA and vPykA revealed that the 333 N-terminal amino acids are highly conserved with 78% identity, whereas the C-terminal domains are less conserved (Figure 13). Therefore, we assumed that the C-terminal domain of vPykA might determine binding specificity for vHPr. To explore the determinant of the species-specific interaction between PykA and HPr and verify our assumption, two chimeric PKs were constructed via a domain-swapping approach. The vePykA protein was made by fusing the N-terminal domain (amino acids 1-333) of vPykA to the C-terminal domain (amino acids 334-480) of ePykA, whereas the evPykA protein consisted of the N-terminal

domain (amino acids 1-318) of ePykA and the C-terminal domain (amino acids 319-482) of vPykA. The sequences of all the constructs were confirmed by DNA sequencing. After partial purification, each chimeric PK was mixed with a fixed amount of H-vHPr and subjected to pull-down assays using TALON metal affinity resin. When vePykA and ePykA were mixed with H-vHPr, no interaction was detected (Figure 14, lane 3, 4, 7 and 8). In contrast, when vPykA and evPykA were incubated with H-vHPr, they were pulled down by TALON resin (Figure 14, lane 1, 2, 5 and 6). These results led us to conclude that the C-terminal domain of vPykA determines the binding specificity of the vHPr-vPykA complex.

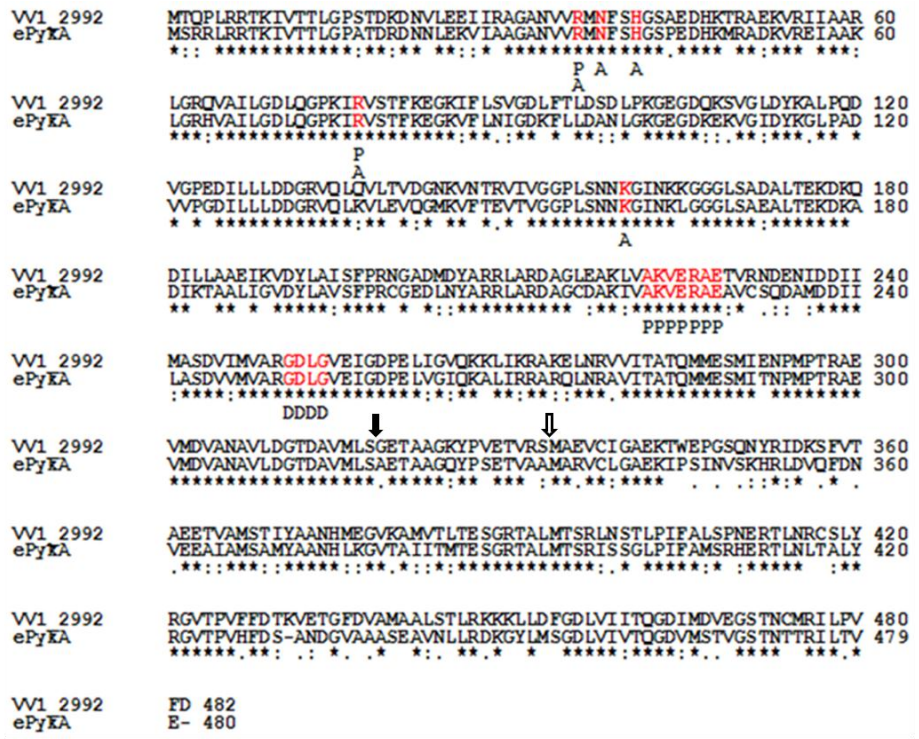

	N-terminal domain (1-333)	C-terminal domain (334-482)
% Identity	78	57

Figure 13. Construction and purification of domain-swapped PKs.

The alignment of amino acid sequences of vPykA (VV1_2992) and ePykA. Sequences were aligned using ClustalW software. The letters A, P, and D below indicate binding sites for ATP, PEP, and divalent cations, respectively. Two chimeric PKs (evPykA, vePykA) were constructed via domain swapping between vPykA and vPykA as described in the Materials and Methods to determine the domain that is involved in the species-specific interaction. Amino acid sites at the domain transition used for domain swapping are indicated with arrows: black for evPykA and white for vePykA. Percent amino acid sequence identities of N-terminal and C-terminal domains of vPykA and ePykA were obtained using BLAST.

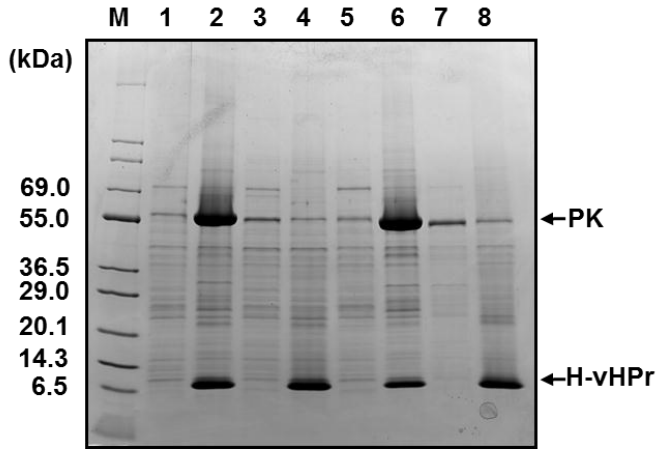

Figure 14. Test for the interaction between chimeric PKs and vHPr. After partial purification, vPykA (lane 1 and 2), vePykA (lane 3 and 4), evPykA (lane 5 and 6), and ePykA (lane 7 and 8) were subjected TALON affinity chromatography in the absence (odd-numbered lanes) and presence (even-numbered lanes) of H-vHPr. Lane M, molecular mass markers (Koma Biotech, Inc.).

2. Effect of vHPr on vPykA activity

2.1. Allosteric effect between PKs and HPr proteins

Because the binding site for the allosteric effector is located at the C-terminal domain of PKs (Jurica *et al.*, 1998, Larsen *et al.*, 1994) and the C-terminal domain determines the specificity of the HPr-PykA interaction, we tested whether HPr can act as an allosteric regulator of PykA. PK activity was determined by a lactate dehydrogenase (LDH)-coupled assay that measures the decrease in absorbance at 340 nm resulting from the oxidation of NADH to NAD^+. This assay is based on the conversion of PEP to pyruvate by PK, coupled to the conversion of pyruvate to lactate by LDH at the expense of NADH (Zoraghi *et al.*, 2010).

To investigate whether the specific interaction of HPr and PykA is directly related to the specific regulation of PK activity, four different PKs (vPykA, evPykA, vePykA, and ePykA) were purified (Figure 15A), and their activities were compared in the presence and absence of eHPr or vHPr (Figure 15B and C). vPykA demonstrated approximately the same specific activity as ePykA. However, the chimeric protein vePykA comprising an N-terminal two-thirds from vPykA linked to a C-terminal one-third from ePykA exhibited a significantly lower specific activity, whereas evPykA consisting of an N-terminal two-

thirds from ePykA and a C-terminal one-third from vPykA showed a considerably higher specific activity than that of vPykA and ePykA. As expected from the binding assays (Figure 12), ePykA activity was little affected by either eHPr or vHPr, whereas vPykA activity was significantly stimulated by vHPr. eHPr also stimulated vPykA activity, albeit to a much lesser degree than vHPr (Figure 15B). Notably, the enzyme activity of vePykA was not stimulated by either eHPr or vHPr, whereas evPykA behaved in a manner similar to vPykA in terms of activity regulation by vHPr and eHPr (Figure 15C). These results are in accordance with the data from the binding assays (Figure 12 and 14) and indicate that HPr stimulates enzyme activity by binding to the allosteric site in the C-terminal domain of vPykA.

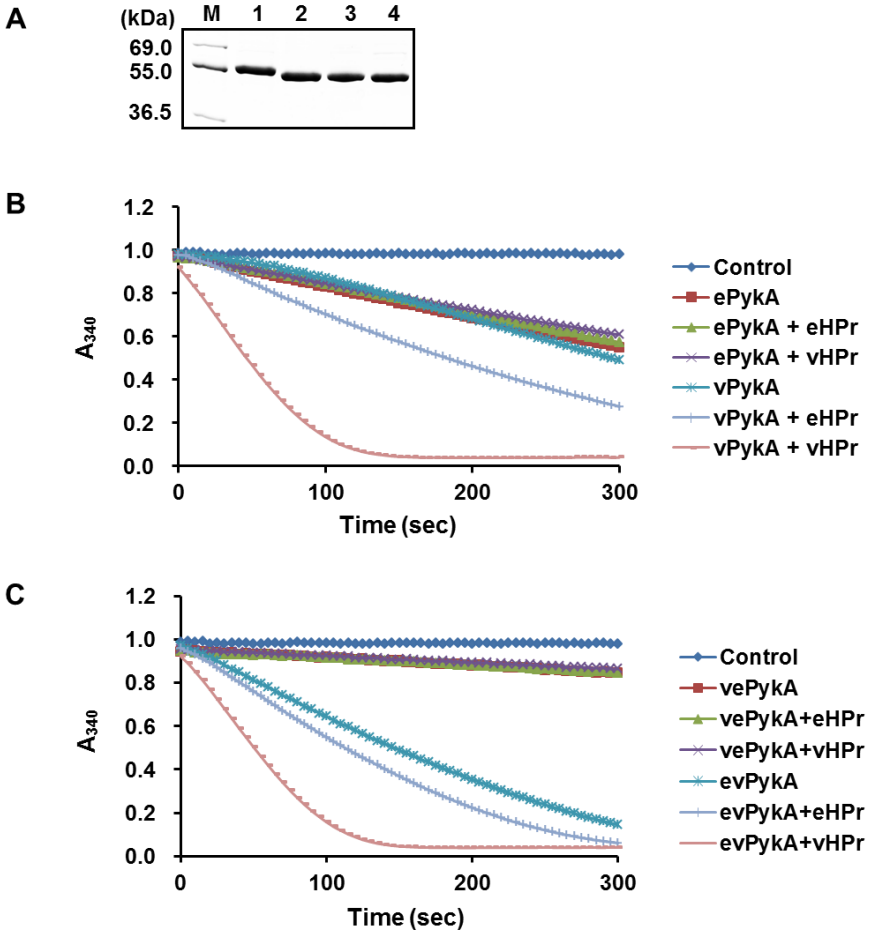
A
(kDa)
M
1
2
3
4
69.0
55.0
36.5
B
1.2
1.0
0.8
0.6
0.4
0.2
0.0
A340
0
100
200
300
Time (sec)
Control
ePykA
ePykA + eHPr
ePykA + vHPr
vPykA
vPykA + eHPr
vPykA + vHPr
C
1.2
1.0
0.8
0.6
0.4
0.2
0.0
A340
0
100
200
300
Time (sec)
Control
vePykA
vePykA+eHPr
vePykA+vHPr
evPykA
evPykA+eHPr
evPykA+vHPr

Figure 15. Test for the allosteric effect between PKs and HPr proteins.

A. Four different PKs were purified and analyzed by SDS-PAGE followed by staining with Coomassie brilliant blue (2 μg each): lane 1, vPykA; lane 2, vePykA; lane 3, evPykA; lane 4, ePykA. Lane M, molecular mass markers (Koma Biotech, Inc.).

B and C. The rates of PEP conversion to pyruvate catalyzed by four different PKs (native forms of ePykA and vPykA in (B) and two domain-swapped PKs in (C), 20 nM each) were measured by a lactate dehydrogenase (LDH)-coupled assay in the presence of 20 μM of eHPr or vHPr as indicated.

2.2. The phosphorylation state of vHPr is important for the regulation of vPykA activity

vPykA activity was determined in the presence of varying concentrations of AMP, fructose 1,6-bisphosphate (FBP), and vHPr (Figure 16) . As expected given its high sequence identity with ePykA (71%) and low sequence identity with ePykF (37%), vPykA activity was not significantly influenced by FBP. Interestingly, however, vPykA was activated by 8 mM AMP by only approximately two-fold, whereas ePykA was activated more than 10-fold (Figure 16A). Dephospho-vHPr increased vPykA activity in a concentration-dependent manner up to approximately 7-fold compared to the level in control assays (Figure 16B). From these data, it can be assumed that the *in vivo* allosteric effector of vPykA might be dephospho-vHPr rather than AMP. The stimulation of vPykA activity by dephospho-vHPr was saturable, with maximal activation at 16 μM of vHPr and half-maximal activation at approximately 4 μM.

It was previously shown that eHPr interacts with glycogen phosphorylase (GP) in *E. coli* and increases GP activity to 250% of the level in control assays (Seok *et al.*, 1997a). In addition, while phosphorylated eHPr (P-eHPr) was shown to have about four-times higher affinity toward GP than the dephosphorylated form of eHPr,

dephospho-eHPr activates GP more than the phosphorylated form. We therefore investigated the effect of the phosphorylation state of vHPr on the regulation of vPykA activity. To determine if phosphorylation of vHPr would affect its stimulatory activity, PEP (1 mM), EI (2 μg/ml), and variable concentrations of vHPr were added to a coupled enzyme assay. This reaction mixture was preincubated for 5 min before the assay was initiated by the addition of vPykA. Notably, the addition of phospho-vHPr resulted in no stimulation of vPykA activity regardless of the amount of vHPr, indicating that only dephospho-vHPr can interact with and thus stimulate the activity of vPykA.

To evaluate the effect of vHPr on the catalytic function of vPykA, steady-state kinetics of vPykA were determined with respect to PEP in the absence and presence of 20 μM dephospho-vHPr (Figure 17). Parameters derived from these kinetics are summarized in Table 3. While vHPr showed little, if any, effect on the V_{max}, Hill coefficient (h) and catalytic activity (k_{cat}) of vPykA, the presence of vHPr led to an approximately 3.7-fold decrease in the $S_{0.5}$ of PEP under nonsaturation conditions. These data imply that the phosphorylation state of vHPr regulates vPykA activity by influencing the affinity of vPykA for PEP.

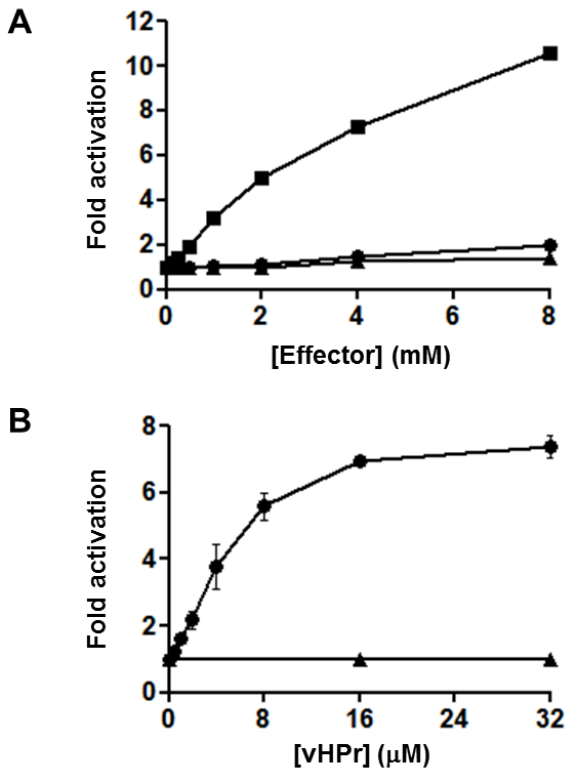

Figure 16. The allosteric regulation of vPykA.

A. Effects of varying concentrations of AMP (0-8 mM) on ePykA (squares) and vPykA (circles) activity. The effects of various concentrations of fructose 1,6-bisphosphate (0-8 mM) on vPykA (triangles) were also measured.

B. The effects of varying amounts of dephospho-vHPr (circles) and phospho-vHPr (triangles) on vPykA activity. The results are presented as the mean ± standard deviations (n = 3).

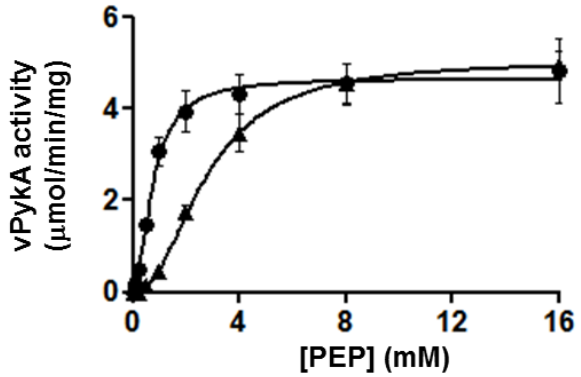

Figure 17. Steady-state kinetics of vPykA in the absence and presence of vHPr.

Steady-state kinetics of vPykA were determined with respect to PEP (0-16 mM) in the absence (triangles) and presence (circles) of 20 μM dephospho-vHPr. vPykA and ePykA were added to 20 nM. The results are presented as the mean ± standard deviations (n = 3). The resultant kinetic parameters are presented in Table 3.

Table 3. Kinetic parameters of vPykA with respect to PEP in the presence and absence of vHPr.

	- vHPr	+ vHPr
V_{max} (μmol min^{-1} mg^{-1})	5.04 ± 0.14	4.66 ± 0.14
h	2.16 ± 0.18	1.86 ± 0.23
$S_{0.5}$ (mM)	2.74 ± 0.14	0.74 ± 0.06
k_{cat} (sec^{-1})	4.31 ± 0.12	3.98 ± 0.12

3. *In vivo* effect of the vHPr–vPykA interaction

3.1. The *in vivo* phosphorylation state of vHPr

It is generally accepted that the phosphorylation states of the PTS proteins vary according to the availability of PTS substrates and the metabolic state of the cell (Deutscher *et al.*, 2014). Indeed, it has recently been revealed that eHPr is almost completely dephosphorylated in LB medium supplemented with the PTS sugar glucose, whereas it exists mainly in the phosphorylated form in LB medium supplemented with a non-PTS sugar in *E. coli*. To determine whether the phosphorylation state of vHPr also depends on the availability of a PTS sugar, we measured the phosphorylation level of vHPr in cells grown in LB medium containing 2.5% NaCl (LBS) supplemented with either glucose or galactose. As shown in Figure 18, vHPr was mostly dephosphorylated in LBS medium supplemented with glucose, whereas it was predominantly in the phosphorylated state in LBS medium and LBS medium supplemented with galactose. Therefore, it could be assumed that vHPr regulates vPykA activity in response to the availability of a preferred PTS sugar, which determines the phosphorylation state of vHPr.

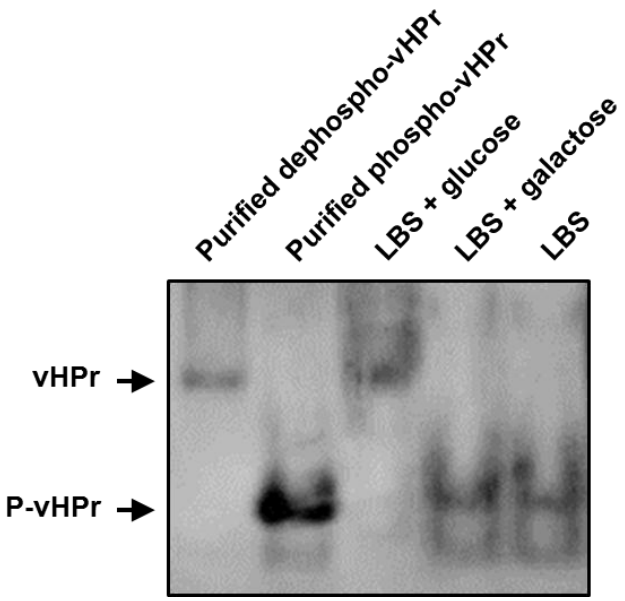

Figure 18. The *in vivo* phosphorylation state of vHPr in the presence of different carbon compounds.

The *in vivo* phosphorylation states of vHPr were determined in CMCP6/pRK-vHPr cells growing exponentially in LBS and LBS containing the indicated. Native PAGE and Western blot analysis were performed following the procedure developed to determine the *in vivo* phosphorylation state of eHPr (Park *et al.*, 2013).

3.2. Phosphorylation state-dependent effect of vHPr on vPykA activity is dependent on the presence of glucose

To confirm the phosphorylation state-dependent effect of vHPr on vPykA activity *in vivo*, we measured the intracellular concentrations of PEP and pyruvate in wild-type CMCP6 and *pykA* mutant cells grown on glucose or galactose after the addition of respective carbon sources. In the wild-type strain, the pyruvate concentration drastically increased with a concomitant decrease in the PEP concentration within 5 min after the addition of 10 mM glucose (Figure 19A and B). Notably, the pyruvate concentration also increased in *pykA* deletion mutant cells after the addition of glucose, but to a considerably lesser extent than in wild-type cells, with a slight decrease in the PEP concentration. In the *pykA* mutant strain transformed with the plasmid pRK-PKA in which vPykA expression is under the control of its own promoter, the pyruvate concentration increased to a similar (or slightly higher) level to that of the wild-type strain, with only a slight decrease in the PEP level after the addition of 10 mM glucose. However, the addition of the non-PTS sugar galactose did not cause any remarkable changes in the intracellular concentrations of pyruvate and PEP in all three strains (Figure 19C and D). It should be noted that the significant difference in the pyruvate concentrations depending on the carbon source was not

due to the differential effects of the two sugars on *pykA* expression in *V. vulnificus* (Figure 20). Therefore, our data suggest that vPykA plays, at least in part, a role in the regulation of the cellular levels of pyruvate by interacting with dephospho-vHPr, which increases in the presence of PTS substrates.

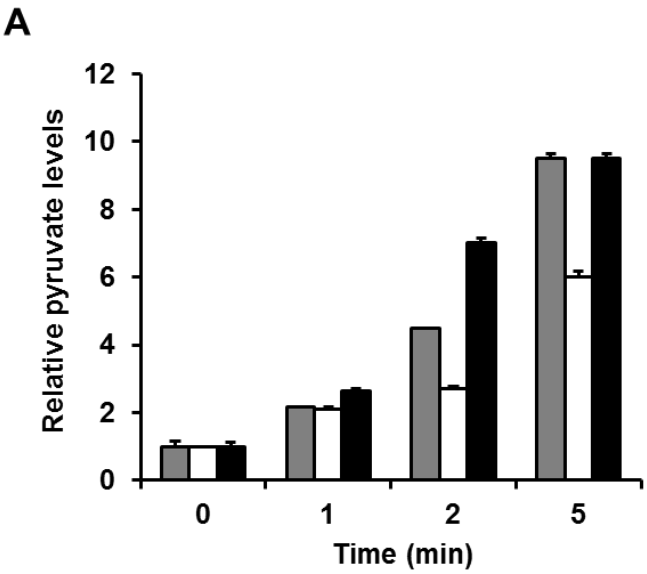
A
Relative pyruvate levels
12
10
8
6
4
2
0
0
1
2
5
Time (min)

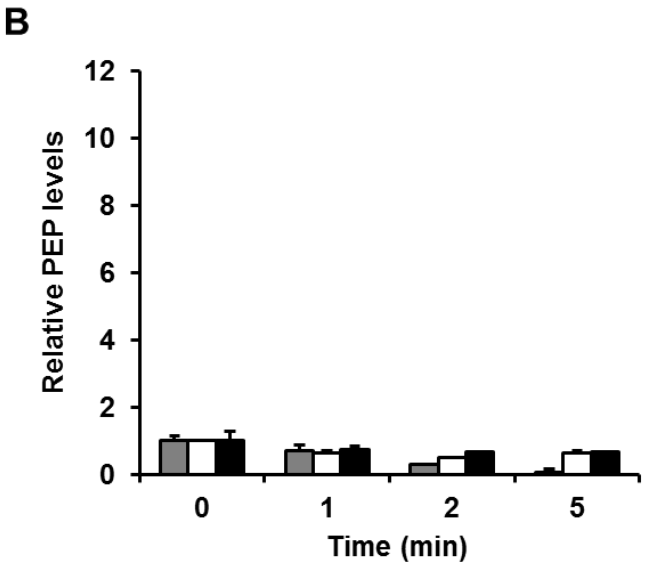
B
Relative PEP levels
12
10
8
6
4
2
0
0
1
2
5
Time (min)

C

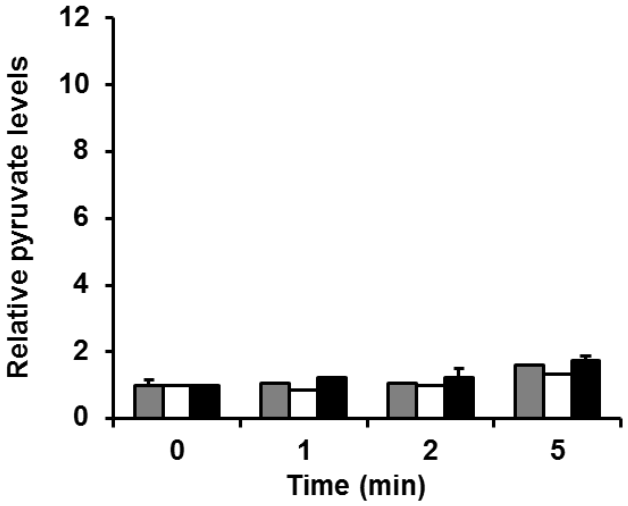
12
10
8
6
4
2
0
Relative pyruvate levels
0
1
2
5
Time (min)

D

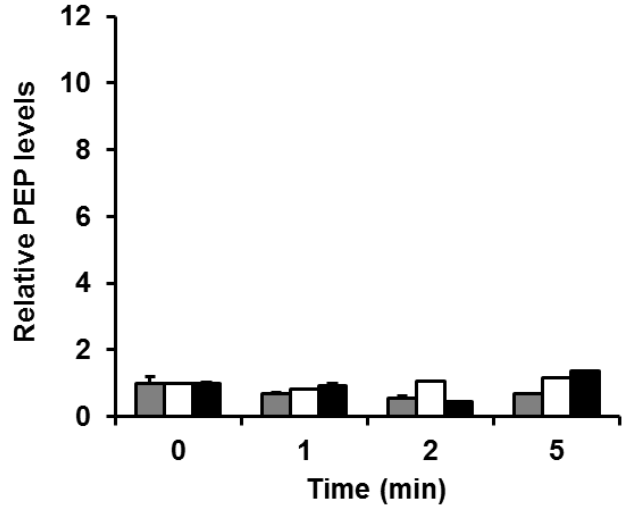
12
10
8
6
4
2
0
Relative PEP levels
0
1
2
5
Time (min)

Figure 19. Changes in the intracellular concentrations of PEP and pyruvate after the addition of glucose or galactose.

A-D. The intracellular concentrations of pyruvate (A and C) and PEP (B and D) were measured as described in the Materials and Methods. Samples were prepared from wild-type CMCP6 (gray bars), the *pykA* deletion mutant (white bars) and the *pykA* deletion mutant harboring a vPykA expression vector (black bars) at the indicated time points after the addition of 10 mM glucose (A and B) or galactose (C and D). The results are presented as the mean ± standard deviations (n = 3).

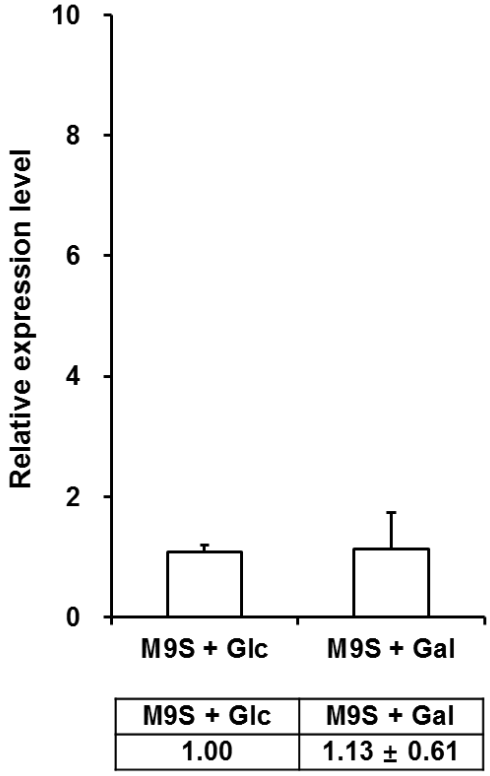

M9S + Glc	M9S + Gal
1.00	1.13 ± 0.61

Figure 20. The relative expression levels of VV1_2992 in the presence of glucose (Glc) or galactose (Gal) by quantitative RT-PCR (qRT-PCR).

Relative expression levels of VV1_2992 were determined by quantitative RT-PCR in wild-type CMCP6 grown in M9S containing 0.2% glucose or galactose. The results are presented as the relative levels (mean ± S.D. of triplicate determinations) compared to the transcript level of VV1_2992 in the presence of glucose.

3.3. Phenotypes of *pykA* deletion mutant

The *pykA* deletion mutant exhibited a distinct growth phenotype. When cells from culture stocks were inoculated into fresh medium after storage at low temperatures, the *pykA* mutant demonstrated much longer lag times than wild-type CMCP6 (Figure 21A). However, subcultures of the mutant exhibited growth similar to that of the wild-type strain (Figure 21B). It is known that, like many other Gram-negative bacteria, *V. vulnificus* is induced into a viable but nonculturable (VBNC) state by incubation at low temperatures (Oliver, 2010). While *V. vulnificus* is easily isolated from both water and shellfish in estuaries during warm months, its isolation during cold months has proved difficult (Whitesides & Oliver, 1997). This decrease in culturability is known to be due to the entrance of this bacterium into the VBNC state.

Therefore, we investigated whether the longer lag observed for the *pykA* mutant stored at low temperatures is related to the VBNC state. As shown in Figure 21C, the *pykA* mutant cells entered the VBNC state much faster than wild-type cells when 5 x 10^6 cells of each of the two strains were incubated in LBS at 4 ℃. Few culturable cells of the mutant were detected at 13 days, while more than 100 colonies of the wild-type strain were formed. Introduction of a plasmid carrying the

wild-type *pykA* gene (pRK-PKA) into the mutant strain rescued the VBNC state to the wild-type level, indicating that the faster entry of the mutant into the VBNC state is solely due to loss of vPykA.

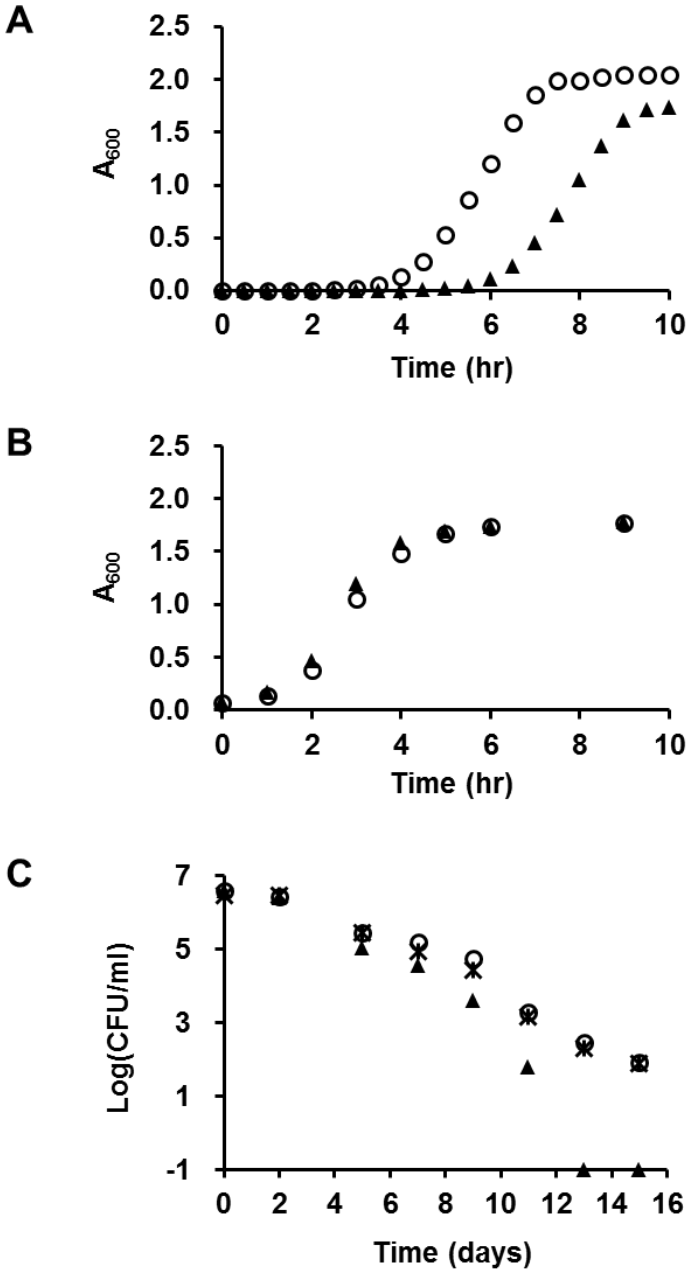
A
2.5
2.0
1.5
1.0
0.5
0.0
A_{600}
0
2
4
6
8
10
Time (hr)
B
2.5
2.0
1.5
1.0
0.5
0.0
A_{600}
0
2
4
6
8
10
Time (hr)
C
7
5
3
1
-1
Log(CFU/ml)
0
2
4
6
8
10
12
14
16
Time (days)

Figure 21. Comparison of growth rates and culturability of wild-type *V. vulnificus* CMCP6 and a *pykA* deletion mutant.

A. Growth curves of cells from frozen culture stocks of wild-type CMCP6 (circles) and the *pykA* deletion mutant (triangles). The culture stocks were diluted with LBS and inoculated into fresh LBS medium at a starting A_{600} of 0.001. Cells were grown aerobically at 30 ℃ with shaking at 200 rpm in LBS medium.

B. Growth curves of subcultures of wild-type CMCP6 (circles) and the *pykA* deletion mutant (triangles). Cells of the two strains grown to stationary phase in (A) were inoculated into fresh LBS medium at a starting A_{600} of 0.01.

C. Effect of vPykA on the culturability of *V. vulnifucus* following incubation at 4 ℃. Log-phase wild-type CMCP6 cells (circles), the *pykA* deletion mutant (triangles) and the *pykA* deletion mutant harboring a vPykA expression vector (asterisks) were incubated at 4 ℃. Aliquots were then plated onto LBS agar plates at the indicated time points and incubated overnight at 30 ℃ to determine culturability. All experiments were performed in biological triplicate.

3.4. vPykA activity confers resistance to H_2O_2

Several studies have provided evidence for the involvement of reactive oxygen species (ROS) in the VBNC state of *V. vulnificus* by showing that a significant portion of the VBNC population of *V. vulnificus* can be resuscitated if catalase or pyruvate is present in the culture medium (Bogosian *et al.*, 2000, Kong *et al.*, 2004, Troxell *et al.*, 2014). Because both catalase and pyruvate are known to eliminate H_2O_2, one explanation for the faster entry of the mutant into the VBNC state might be that decreased production of pyruvate does limit resistance to H_2O_2 which can be generated during normal metabolism and the autoclaving of rich medium. This possibility was tested by comparing the H_2O_2 sensitivity of the mutant with that of wild type cells. While the two strains did not show any difference in growth on LBS medium, the mutant exhibited significantly decreased survival on the same medium but in the presence of 0.25 mM H_2O_2 (Figure 22A). It should be noted that neither of these strains exhibited any growth defect on medium supplemented with pyruvate together with H_2O_2. The mutant strain harboring the pRK-PKA plasmid recovered H_2O_2 resistance to the wild-type level, indicating that the increased sensitivity of the mutant to H_2O_2 was a direct reflection of loss of vPykA.

To confirm whether dephosphorylated vHPr affects resistance to H_2O_2 through an interaction with vPykA *in vivo*, we constructed pRK-H15A, a vector expressing an unphosphorylatable form of vHPr (H15A), and pRK-PKA&H15A, a vector coexpressing vPykA and vHPr (H15A). As shown in Figure 22B, the mutant strain with pRK-PKA was more resistant to H_2O_2 than the mutant carrying pRK-H15A, whereas the mutant carrying pRK-PKA&H15A was even more resistant than the strain carrying pRK-PKA.

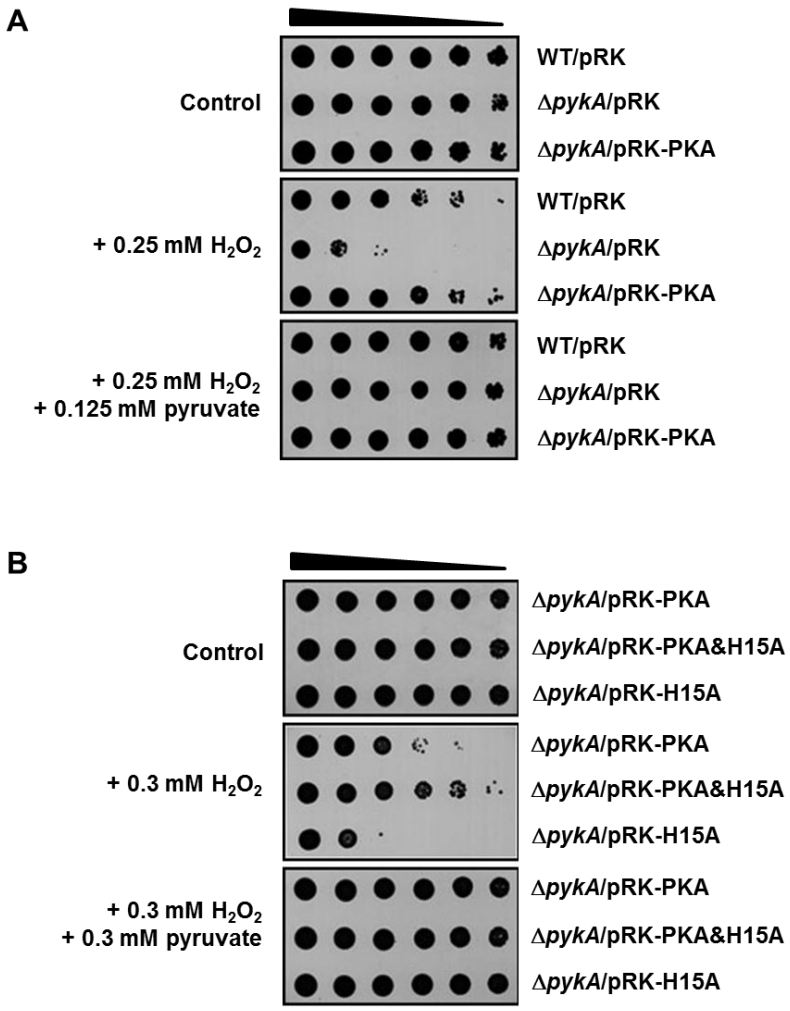

Figure 22. Effects of vPykA activity and pyruvate on resistance to H_2O_2.

A and B. Stationary-phase cells of the indicated strains were serially diluted four-fold from 0.25 x 10^8 cells ml^{-1} (A) or 10^8 cells ml^{-1} (B), and 2-μl aliquots were spotted onto LBS agar plates containing different combinations of H_2O_2 and pyruvate as indicated. After incubation at 30 ℃ for 24 h, the plates were scanned.

Based on these data, it can be assumed that vHPr regulates vPykA activity in response to the availability of a preferred sugar, which determines the phosphorylation state of vHPr. Thus, we tested the effect of sugars on the H_2O_2 sensitivity of the *pykA* mutant with that of wild type cells. The two strains did not show any difference in growth on M9 minimal medium containing 0.2% casamino acids and 2.5% NaCl (M9S) supplemented with galactose or glucose, the mutant exhibited significantly decreased survival on the same medium but in the presence of 0.125 mM H_2O_2 (Figure 23). None of these strains exhibited any growth defect on the medium supplemented with pyruvate together with H_2O_2. The mutant strain harboring the pRK-PKA plasmid recovered H_2O_2 resistance to the wild-type level. Interestingly, while the sensitivity of the mutant strain to H_2O_2 was little affected by sugar source added to M9S medium, the wild-type strain exhibited a markedly less sensitivity to H_2O_2 in M9S containing glucose than in M9S containing galactose. Because vHPr exists mainly in the dephosphorylated form in the presence of glucose but in the phosphorylated form in the presence of galactose (Figure 18), we assumed that higher resistance to H_2O_2 displayed by glucose-grown cells may be due, at least in part, to increased activation of vPykA by dephospho-vHPr. Therefore, it seems likely that dephosphorylated

vHPr interacts with vPykA *in vivo* and activates vPykA-mediated pyruvate production to confer resistance to H_2O_2 stress in the presence of a PTS sugar, such as glucose.

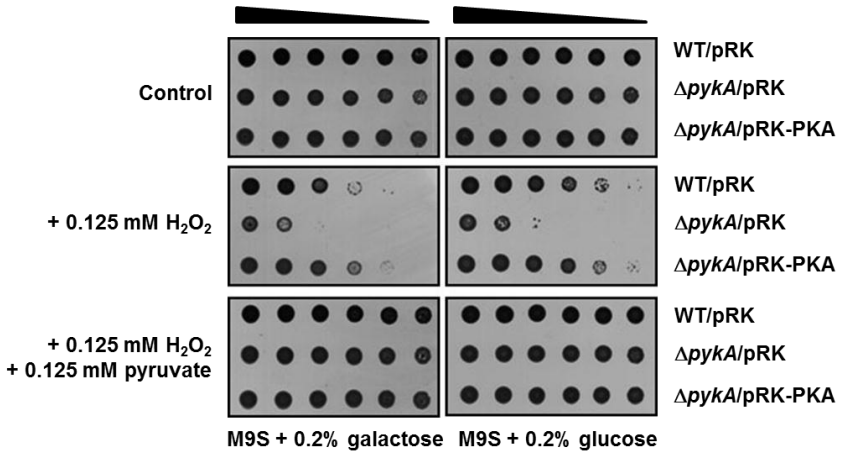

Figure 23. Effects of vPykA activity and sugars on resistance to H_2O_2.

Stationary-phase cells of the indicated strains were serially diluted four-fold from 10^8 cells ml^{-1}, and 2-μl aliquots were spotted onto M9S agar plates containing different combinations of carbon sources, H_2O_2 and pyruvate as indicated. After incubation at 30 ℃ for 24 h, the plates were scanned.

4. The essentiality of the gene coding for the vPykF

Despite several attempts, we failed to obtain a deletion mutant of *vpykF*. The essentiality of this gene was proven by using a conditional knock-out strain in which the gene was placed under the control of a conditionally expressed promoter. In this experiment, chromosomal *vpykF* null mutation was complemented by pJK1113 plasmid containing the *ara*C-P_{BAD} promoter and *vpykF* gene. The viability of the mutant depends on the presence of arabinose to induce the expression of the corresponding gene (Figure 24). The *ara*C-P_{BAD} promoter system provided efficient repression of *vpykF* in glucose such that it failed to produce enough copies of the protein to complement the chromosomal null mutation. These observations indicate that the *vpykF* gene is indeed essential.

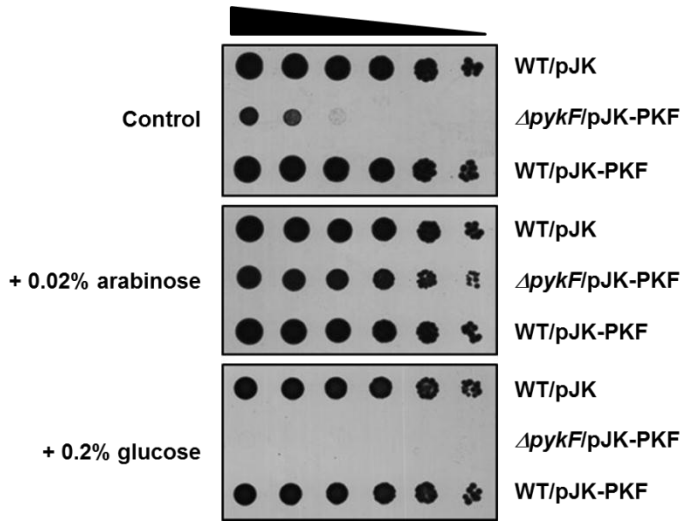

Figure 24. Differential colony formation of *vpykF* mutant strain on arabinose or glucose-containing LB agar plates.

Stationary-phase cells of the indicated strains were serially diluted four-fold from 10^7 cells ml^{-1}, and 2-μl aliquots were spotted onto LBS containing 20 mM sodium phosphate (pH 7.0) agar plates supplemented with arabinose or glucose as indicated. After incubation at 30 ℃ for 24 h, the plates were scanned.

CHAPTER IV. Discussion

Many bacteria including a variety of human pathogens are known to enter the viable but nonculturable (VBNC) state in response to various environmental stresses (Oliver, 2010). Different chemical and environmental factors have been reported to induce the VBNC state depending on the bacterial species. Because H_2O_2 plays a critical role in VBNC in the opportunistic human pathogen *V. vulnificus*, production of hydrogen scavengers such as catalase and pyruvate should be regulated in a highly sophisticated way to promote survival under adverse environmental conditions. Pyruvate kinase (PK) catalyzes the final step of glycolysis, specifically the irreversible conversion of PEP to pyruvate with concomitant phosphorylation of ADP to ATP, whereas the PTS catalyzes the first step of glycolysis, which is the coupled transport and phosphorylation of sugars. Because dephosphorylated forms of the PTS proteins increase during transport of a preferred PTS substrate such as glucose, the PTS also functions as a sensory system for monitoring environmental changes such as nutrient availability. In this study, we provide evidence that vHPr of the PTS stimulates vPykA activity and thereby increases resistance of *V. vulnificus* cells to H_2O_2 by sensing glucose (Figure 25).

The maximal stimulation of vPykA activity by dephospho-vHPr could be obtained at approximately 16 μM of vHPr up to seven-fold

compared to the level in control assays without the addition of vHPr (Figure 16B). The intracellular concentration of HPr was previously calculated to be 20-100 μM in *E. coli* and *Salmonella typhimurium* (Mattoo & Waygood, 1983, Rohwer *et al.*, 2000). Similar to eHPr in *E. coli* cells (Park *et al.*, 2013), vHPr exists mainly in the phosphorylated form in LBS medium and LBS medium supplemented with galactose which is a non-PTS sugar, whereas it is predominantly found in the dephosphorylated state in medium supplemented with glucose which is a PTS sugar in *V. vulnificus* cells (Figure 18). These data suggest that the concentration of dephosphorylated HPr can vary from 0 to 100 μM, and the total activity of vPykA can change up to seven-fold in cells depending on the carbon source. Because this regulation does not occur in *E. coli*, it thus seems likely that the regulatory roles of the PTS reflect species-specific metabolic needs.

It is quite interesting that the regulatory interactions of HPr with its target proteins are species-specific. Despite the fact that both *E. coli* and *V. vulnificus* belong to γ-proteobacteria, and thus orthologous proteins in the two species share high amino acid sequence identity (33% for Rsd, 47% for glycogen phosphorylase, 71% for PykA, and 76% for HPr), we could not detect either Rsd or glycogen phosphorylase from *V.*

vulnificus extracts in repeated ligand fishing experiments using vHPr as bait. While ePykA cannot bind to either eHPr or vHPr, eHPr binds to vPykA and stimulates its activity, albeit to a much lesser degree than does vHPr. Because phosphorylation at His 15 of vHPr abolishes its interaction with vPykA, it could be assumed that the binding surface on vHPr would include amino acid residues near His 15. Comparison of the amino acid sequence of eHPr with that of vHPr indicates that amino acid residues located near His 15 on the three dimensional structure of eHPr are quite well conserved, except for Pro11 and Glu85 (Glu 11 and His85 in vHPr, respectively) (Figure 26A and B). Therefore, the difference in these two residues might, at least in part, explain the lower affinity of eHPr to vPykA. Structural studies on the vHPr-vPykA complex will help to understand the species-specific nature of this regulatory interaction between vHPr and vPykA. It is also interesting that the specific PK activities of the two PykA proteins change reciprocally after swapping the C-domain, where the binding site for the allosteric effector is located. It was previously shown that the allosteric transition between the inactive T-state and the active R-state involved a symmetrical 6° rigid-body rocking motion of the A- and C-domain cores in each of the four subunits to alter tetramer rigidity (Morgan *et al.*, 2010). Therefore, the reciprocal changes in the specific

PK activities of the two PykA proteins after the C-domain swap might be attributable to changes in tetramer rigidity. Structural studies of these hybrid proteins are required to fully understand the mechanisms underlying of this reciprocal activity swap.

PK has been recently identified as an absolutely essential gene for survival of other bacteria such as *H. influenzae*, *Streptococcus pneumoniae*, and *Mycobacterium tuberculosis* using allelic replacement mutagenesis (Akerley *et al.*, 2002, Sassetti *et al.*, 2003, Song *et al.*, 2005, Zhang *et al.*, 2004). The proven essential nature of PK in these bacteria is a very important feature of this enzyme, since products of genes that are essential for viability of the microorganism *in vitro* can be considered as potential drug targets in the effort to develop new classes of antimicrobial agents (Thomson *et al.*, 2004). Here we report the essentiality of vPykF. Gene disruption studies demonstrated vPykF is essential for *V. vulnificus* growth and survival, suggesting that this protein may be a potential drug target.

Although the relative expression levels of vPykA were lower than those of vPykF (Figure 5B), our data revealed that vPykA plays a physiologically important role and appropriate combination of two PKs is necessary for efficient regulation in *V. vulnificus* metabolism.

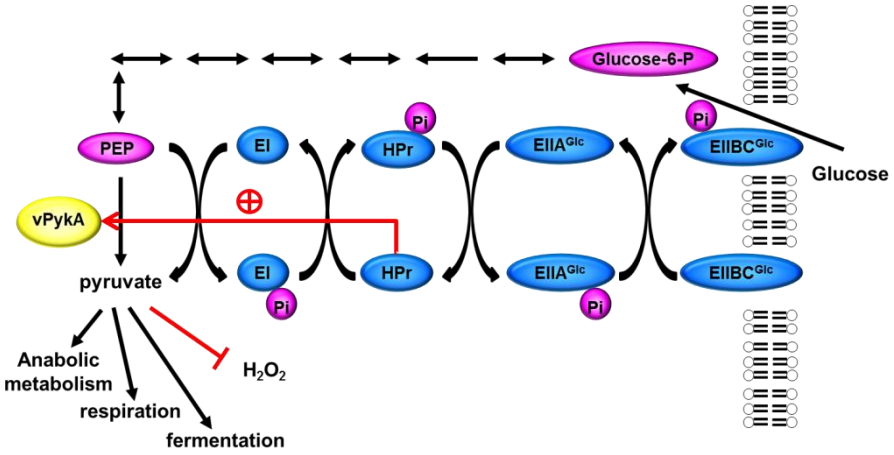

Figure 25. A model for the regulation of PK activity via the interaction between vPykA and vHPr in response to the availability of glucose.

When glucose is phosphorylated during transport, vHPr becomes dephosphorylated. Dephosphorylated vHPr then interacts with vPykA and activates the conversion of PEP to pyruvate. In addition to its role as the key metabolic intermediate in both aerobic and anaerobic metabolism, pyruvate increases the resistance of *V. vulnificus* cells to H_2O_2 stress in the presence of glucose.

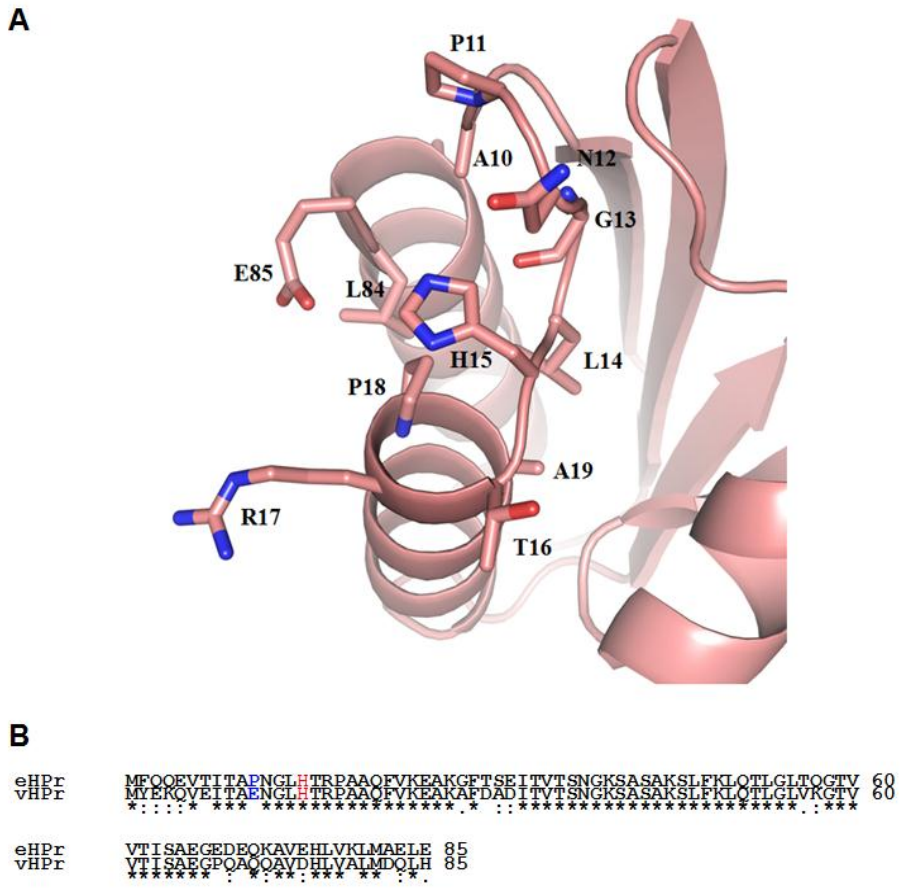

Figure 26. Comparison of eHPr and vHPr.

A. Amino acid residues near the phosphorylation site histidine 15 residue in the 3D structure of eHPr. The image was constructed with PyMOL from PDB 1POH.

B. The alignment of amino acid sequences of eHPr and vHPr using ClustalW software. The histidine 15 residues in the two proteins are marked in red.

CHAPTER V. References

Akerley, B.J., E.J. Rubin, V.L. Novick, K. Amaya, N. Judson & J.J. Mekalanos, (2002) A genome-scale analysis for identification of genes required for growth or survival of *Haemophilus influenzae*. *Proc Natl Acad Sci U S A* **99**: 966-971.

Amaro, C., L.I. Hor, E. Marco-Noales, T. Bosque, B. Fouz & E. Alcaide, (1999) Isolation of *Vibrio vulnificus* serovar E from aquatic habitats in Taiwan. *Appl Environ Microbiol* **65**: 1352-1355.

Besnard, V., M. Federighi, E. Declerq, F. Jugiau & J.M. Cappelier, (2002) Environmental and physico-chemical factors induce VBNC state in *Listeria monocytogenes*. *Vet Res* **33**: 359-370.

Bisharat, N., V. Agmon, R. Finkelstein, R. Raz, G. Ben-Dror, L. Lerner, S. Soboh, R. Colodner, D.N. Cameron, D.L. Wykstra, D.L. Swerdlow & J.J. Farmer, 3rd, (1999) Clinical, epidemiological, and microbiological features of *Vibrio vulnificus* biogroup 3 causing outbreaks of wound infection and bacteraemia in Israel. Israel *Vibrio* Study Group. *Lancet* **354**: 1421-1424.

Bogosian, G., N.D. Aardema, E.V. Bourneuf, P.J. Morris & J.P. O'Neil, (2000) Recovery of hydrogen peroxide-sensitive culturable cells of *Vibrio vulnificus* gives the appearance of resuscitation from a viable but nonculturable state. *J Bacteriol* **182**: 5070-5075.

Bowden, S.D., G. Rowley, J.C. Hinton & A. Thompson, (2009) Glucose and glycolysis are required for the successful infection of macrophages and mice by *Salmonella enterica* serovar typhimurium. *Infect Immun* **77**: 3117-3126.

Bruckner, R. & F. Titgemeyer, (2002) Carbon catabolite repression in bacteria: choice of the carbon source and autoregulatory limitation of sugar utilization. *FEMS Microbiol Lett* **209**: 141-148.

Chang, T.M., Y.C. Chuang, J.H. Su & M.C. Chang, (1997) Cloning and sequence analysis of a novel hemolysin gene (vllY) from *Vibrio vulnificus*. *Appl Environ Microbiol* **63**: 3851-3857.

Chauvin, F., L. Brand & S. Roseman, (1994) Sugar transport by the bacterial phosphotransferase system. Characterization of the *Escherichia coli* enzyme I monomer/dimer transition kinetics by fluorescence anisotropy. *J Biol Chem* **269**: 20270-20274.

Chuang, D.T. & M.F. Utter, (1979) Structural and regulatory properties of pyruvate kinase from *Pseudomonas citronellolis*. *J Biol Chem* **254**: 8434-8441.

Crow, V.L. & G.G. Pritchard, (1982) Pyruvate kinase from *Streptococcus lactis*. *Methods Enzymol* **90 Pt E**: 165-170.

D'Auria, S., M. Rossi, P. Herman & J.R. Lakowicz, (2000) Pyruvate kinase from the thermophilic eubacterium *Bacillus acidocaldarius* as probe to monitor the sodium concentrations in the blood. *Biophys Chem* **84**: 167-176.

Deutscher, J., F.M. Ake, M. Derkaoui, A.C. Zebre, T.N. Cao, H. Bouraoui, T. Kentache, A. Mokhtari, E. Milohanic & P. Joyet, (2014) The bacterial phosphoenolpyruvate:carbohydrate phosphotransferase system: regulation by protein phosphorylation and phosphorylation-dependent protein-protein interactions. *Microbiol Mol Biol Rev* **78**: 231-256.

Deutscher, J., C. Francke & P.W. Postma, (2006) How phosphotransferase system-related protein phosphorylation regulates carbohydrate metabolism in bacteria. *Microbiol Mol Biol Rev* **70**: 939-1031.

Dombrauckas, J.D., B.D. Santarsiero & A.D. Mesecar, (2005) Structural basis for tumor pyruvate kinase M2 allosteric regulation and catalysis. *Biochemistry* **44**: 9417-9429.

Dorschug, M., R. Frank, H.R. Kalbitzer, W. Hengstenberg & J. Deutscher, (1984) Phosphoenolpyruvate-dependent phosphorylation site in enzyme III^{Glc} of the *Escherichia coli* phosphotransferase system. *Eur J Biochem* **144**: 113-119.

Du, M., J. Chen, X. Zhang, A. Li, Y. Li & Y. Wang, (2007) Retention of virulence in a viable but nonculturable *Edwardsiella tarda* isolate. *Appl Environ Microbiol* **73**: 1349-1354.

Ducret, A., M. Chabalier & S. Dukan, (2014) Characterization and resuscitation of 'non-culturable' cells of *Legionella pneumophila*. *BMC Microbiol* **14**: 3.

Emmerling, M., J.E. Bailey & U. Sauer, (1999) Glucose catabolism of *Escherichia coli* strains with increased activity and altered regulation of key glycolytic enzymes. *Metab Eng* **1**: 117-127.

Espat, N.J., T. Auffenberg, A. Abouhamze, J. Baumhofer, L.L. Moldawer & R.J. Howard, (1996) A role for tumor necrosis factor-alpha in the increased mortality associated with *Vibrio vulnificus* infection in the presence of hepatic dysfunction. *Ann Surg* **223**: 428-433.

Fox, D.K., N.D. Meadow & S. Roseman, (1986) Phosphate transfer between acetate kinase and enzyme I of the bacterial phosphotransferase system. *J Biol Chem* **261**: 13498-13503.

Gander, R.M. & M.T. LaRocco, (1989) Detection of piluslike structures on clinical and environmental isolates of *Vibrio vulnificus*. *J Clin Microbiol* **27**: 1015-1021.

Garcia-Alles, L.F., A. Zahn & B. Erni, (2002) Sugar recognition by the glucose and mannose permeases of *Escherichia coli*. Steady-state kinetics and inhibition studies. *Biochemistry* **41**: 10077-10086.

Garcia-Olalla, C. & A. Garrido-Pertierra, (1987) Purification and kinetic properties of pyruvate kinase isoenzymes of *Salmonella typhimurium*. *Biochem J* **241**: 573-581.

Gray, L.D. & A.S. Kreger, (1985) Purification and characterization of an extracellular cytolysin produced by *Vibrio vulnificus*. *Infect Immun* **48**: 62-72.

Guzman, L.M., D. Belin, M.J. Carson & J. Beckwith, (1995) Tight regulation, modulation, and high-level expression by vectors containing the arabinose PBAD promoter. *J Bacteriol* **177**: 4121-4130.

Heidelberg, J.F., M. Shahamat, M. Levin, I. Rahman, G. Stelma, C. Grim & R.R. Colwell, (1997) Effect of aerosolization on culturability and viability of gram-negative bacteria. *Appl Environ Microbiol* **63**: 3585-3588.

Hogema, B.M., J.C. Arents, R. Bader, K. Eijkemans, H. Yoshida, H. Takahashi, H. Aiba & P.W. Postma, (1998) Inducer exclusion in *Escherichia coli* by non-PTS substrates: the role of the PEP

to pyruvate ratio in determining the phosphorylation state of enzyme IIA^{Glc}. *Mol Microbiol* **30**: 487-498.

Holtman, C.K., A.C. Pawlyk, N.D. Meadow & D.W. Pettigrew, (2001) Reverse genetics of *Escherichia coli* glycerol kinase allosteric regulation and glucose control of glycerol utilization *in vivo*. *J Bacteriol* **183**: 3336-3344.

Houot, L., S. Chang, C. Absalon & P.I. Watnick, (2010) *Vibrio cholerae* phosphoenolpyruvate phosphotransferase system control of carbohydrate transport, biofilm formation, and colonization of the germfree mouse intestine. *Infect Immun* **78**: 1482-1494.

Hultquist, D.E., (1968) The preparation and characterization of phosphorylated derivatives of histidine. *Biochim Biophys Acta* **153**: 329-340.

Hurley, J.H., H.R. Faber, D. Worthylake, N.D. Meadow, S. Roseman, D.W. Pettigrew & S.J. Remington, (1993) Structure of the regulatory complex of *Escherichia coli* III^{Glc} with glycerol kinase. *Science* **259**: 673-677.

Iliffe-Lee, E.R. & G. McClarty, (2002) Pyruvate kinase from *Chlamydia trachomatis* is activated by fructose-2,6-bisphosphate. *Mol Microbiol* **44**: 819-828.

Jeong, J.Y., Y.J. Kim, N. Cho, D. Shin, T.W. Nam, S. Ryu & Y.J. Seok, (2004) Expression of *ptsG* encoding the major glucose transporter is regulated by ArcA in *Escherichia coli*. *J Biol Chem* **279**: 38513-38518.

Jurica, M.S., A. Mesecar, P.J. Heath, W. Shi, T. Nowak & B.L. Stoddard, (1998) The allosteric regulation of pyruvate kinase by fructose-1,6-bisphosphate. *Structure* **6**: 195-210.

Kapoor, R. & T.A. Venkitasubramanian, (1983) Purification and properties of pyruvate kinase from *Mycobacterium smegmatis*. *Arch Biochem Biophys* **225**: 320-330.

Kaspar, C.W. & M.L. Tamplin, (1993) Effects of temperature and salinity on the survival of *Vibrio vulnificus* in seawater and shellfish. *Appl Environ Microbiol* **59**: 2425-2429.

Keen, N.T., S. Tamaki, D. Kobayashi & D. Trollinger, (1988) Improved broad-host-range plasmids for DNA cloning in gram-negative bacteria. *Gene* **70**: 191-197.

Kim, H.J., C.R. Lee, M. Kim, A. Peterkofsky & Y.J. Seok, (2011) Dephosphorylated NPr of the nitrogen PTS regulates lipid A biosynthesis by direct interaction with LpxD. *Biochem Biophys Res Commun* **409**: 556-561.

Kim, Y.J., Y. Ryu, B.M. Koo, N.Y. Lee, S.J. Chun, S.J. Park, K.H. Lee & Y.J. Seok, (2010) A mammalian insulysin homolog is regulated by enzyme IIA^{Glc} of the glucose transport system in *Vibrio vulnificus*. *FEBS Lett* **584**: 4537-4544.

Kim, Y.R., S.E. Lee, C.M. Kim, S.Y. Kim, E.K. Shin, D.H. Shin, S.S. Chung, H.E. Choy, A. Progulske-Fox, J.D. Hillman, M. Handfield & J.H. Rhee, (2003) Characterization and pathogenic significance of *Vibrio vulnificus* antigens preferentially expressed in septicemic patients. *Infect Immun* **71**: 5461-5471.

Kimata, K., Y. Tanaka, T. Inada & H. Aiba, (2001) Expression of the glucose transporter gene, *ptsG*, is regulated at the mRNA degradation step in response to glycolytic flux in *Escherichia coli*. *EMBO J* **20**: 3587-3595.

Klontz, K.C., S. Lieb, M. Schreiber, H.T. Janowski, L.M. Baldy & R.A. Gunn, (1988) Syndromes of *Vibrio vulnificus* infections. Clinical and epidemiologic features in Florida cases, 1981-1987. *Ann Intern Med* **109**: 318-323.

Koenig, K.L., J. Mueller & T. Rose, (1991) *Vibrio vulnificus*. Hazard on the half shell. *West J Med* **155**: 400-403.

Kong, I.S., T.C. Bates, A. Hulsmann, H. Hassan, B.E. Smith & J.D. Oliver, (2004) Role of catalase and *oxyR* in the viable but

nonculturable state of *Vibrio vulnificus*. *FEMS Microbiol Ecol* **50**: 133-142.

Koo, B.M., M.J. Yoon, C.R. Lee, T.W. Nam, Y.J. Choe, H. Jaffe, A. Peterkofsky & Y.J. Seok, (2004) A novel fermentation/respiration switch protein regulated by enzyme IIA^{Glc} in *Escherichia coli*. *J Biol Chem* **279**: 31613-31621.

Kubota, Y., S. Iuchi, A. Fujisawa & S. Tanaka, (1979) Separation of four components of the phosphoenolpyruvate: glucose phosphotransferase system in *Vibrio parahaemolyticus*. *Microbiol Immunol* **23**: 131-146.

Kundig, W., S. Ghosh & S. Roseman, (1964) Phosphate Bound to Histidine in a Protein as an Intermediate in a Novel Phospho-Transferase System. *Proc Natl Acad Sci U S A* **52**: 1067-1074.

Larsen, T.M., L.T. Laughlin, H.M. Holden, I. Rayment & G.H. Reed, (1994) Structure of rabbit muscle pyruvate kinase complexed with Mn^{2+}, K^{+}, and pyruvate. *Biochemistry* **33**: 6301-6309.

LaVallie, E.R., E.A. DiBlasio, S. Kovacic, K.L. Grant, P.F. Schendel & J.M. McCoy, (1993) A thioredoxin gene fusion expression system that circumvents inclusion body formation in the *E. coli* cytoplasm. *Biotechnology* **11**: 187-193.

Le Bras, G. & J.R. Garel, (1993) Pyruvate kinase from *Lactobacillus bulgaricus*: possible regulation by competition between strong and weak effectors. *Biochimie* **75**: 797-802.

Lee, C.R., S.H. Cho, M.J. Yoon, A. Peterkofsky & Y.J. Seok, (2007) *Escherichia coli* enzyme IIA^{Ntr} regulates the K^+ transporter TrkA. *Proc Natl Acad Sci U S A* **104**: 4124-4129.

Lee, C.R., Y.H. Park, M. Kim, Y.R. Kim, S. Park, A. Peterkofsky & Y.J. Seok, (2013) Reciprocal regulation of the autophosphorylation of enzyme I^{Ntr} by glutamine and alpha-ketoglutarate in *Escherichia coli*. *Mol Microbiol* **88**: 473-485.

Lee, K.J., C.S. Jeong, Y.J. An, H.J. Lee, S.J. Park, Y.J. Seok, P. Kim, J.H. Lee, K.H. Lee & S.S. Cha, (2011) FrsA functions as a cofactor-independent decarboxylase to control metabolic flux. *Nat Chem Biol* **7**: 434-436.

Lee, S.J., W. Boos, J.P. Bouche & J. Plumbridge, (2000) Signal transduction between a membrane-bound transporter, PtsG, and a soluble transcription factor, Mlc, of *Escherichia coli*. *EMBO J* **19**: 5353-5361.

Litwin, C.M. & B.L. Byrne, (1998) Cloning and characterization of an outer membrane protein of *Vibrio vulnificus* required for heme

utilization: regulation of expression and determination of the gene sequence. *Infect Immun* **66**: 3134-3141.

Litwin, C.M. & S.B. Calderwood, (1993) Role of iron in regulation of virulence genes. *Clin Microbiol Rev* **6**: 137-149.

Lleo, M.M., S. Pierobon, M.C. Tafi, C. Signoretto & P. Canepari, (2000) mRNA detection by reverse transcription-PCR for monitoring viability over time in an *Enterococcus faecalis* viable but nonculturable population maintained in a laboratory microcosm. *Appl Environ Microbiol* **66**: 4564-4567.

Lux, R., K. Jahreis, K. Bettenbrock, J.S. Parkinson & J.W. Lengeler, (1995) Coupling the phosphotransferase system and the methyl-accepting chemotaxis protein-dependent chemotaxis signaling pathways of *Escherichia coli*. *Proc Natl Acad Sci U S A* **92**: 11583-11587.

Malcovati, M. & G. Valentini, (1982) AMP- and fructose 1,6-bisphosphate-activated pyruvate kinases from *Escherichia coli*. *Methods Enzymol* **90 Pt E**: 170-179.

Mattevi, A., G. Valentini, M. Rizzi, M.L. Speranza, M. Bolognesi & A. Coda, (1995) Crystal structure of *Escherichia coli* pyruvate kinase type I: molecular basis of the allosteric transition. *Structure* **3**: 729-741.

Mattoo, R.L. & E.B. Waygood, (1983) Determination of the levels of HPr and enzyme I of the phosphoenolpyruvate-sugar phosphotransferase system in *Escherichia coli* and *Salmonella typhimurium*. *Can J Biochem Cell Biol* **61**: 29-37.

McPherson, V.L., J.A. Watts, L.M. Simpson & J.D. Oliver, (1991) Physiological effects of the lipopolysaccharide of *Vibrio vulnificus* on mice and rats. *Microbios* **67**: 141-149.

Meadow, N.D., R. Revuelta, V.N. Chen, R.R. Colwell & S. Roseman, (1987) Phosphoenolpyruvate:glycose phosphotransferase system in species of *Vibrio*, a widely distributed marine bacterial genus. *J Bacteriol* **169**: 4893-4900.

Mertins, S., B. Joseph, M. Goetz, R. Ecke, G. Seidel, M. Sprehe, W. Hillen, W. Goebel & S. Muller-Altrock, (2007) Interference of components of the phosphoenolpyruvate phosphotransferase system with the central virulence gene regulator PrfA of *Listeria monocytogenes*. *J Bacteriol* **189**: 473-490.

Milton, D.L., R. O'Toole, P. Horstedt & H. Wolf-Watz, (1996) Flagellin A is essential for the virulence of *Vibrio anguillarum*. *J Bacteriol* **178**: 1310-1319.

Miyoshi, N., C. Shimizu, S. Miyoshi & S. Shinoda, (1987) Purification and characterization of *Vibrio vulnificus* protease. *Microbiol Immunol* **31**: 13-25.

Morgan, H.P., I.W. McNae, M.W. Nowicki, V. Hannaert, P.A. Michels, L.A. Fothergill-Gilmore & M.D. Walkinshaw, (2010) Allosteric mechanism of pyruvate kinase from *Leishmania mexicana* uses a rock and lock model. *J Biol Chem* **285**: 12892-12898.

Muirhead, H., (1990) Isoenzymes of pyruvate kinase. *Biochem Soc Trans* **18**: 193-196.

Munoz, M.E. & E. Ponce, (2003) Pyruvate kinase: current status of regulatory and functional properties. *Comp Biochem Physiol B Biochem Mol Biol* **135**: 197-218.

Nam, T.W., S.H. Cho, D. Shin, J.H. Kim, J.Y. Jeong, J.H. Lee, J.H. Roe, A. Peterkofsky, S.O. Kang, S. Ryu & Y.J. Seok, (2001) The *Escherichia coli* glucose transporter enzyme $IICB^{Glc}$ recruits the global repressor Mlc. *EMBO J* **20**: 491-498.

Nam, T.W., H.I. Jung, Y.J. An, Y.H. Park, S.H. Lee, Y.J. Seok & S.S. Cha, (2008) Analyses of Mlc-IIB^{Glc} interaction and a plausible molecular mechanism of Mlc inactivation by membrane sequestration. *Proc Natl Acad Sci U S A* **105**: 3751-3756.

Noguchi, T., H. Inoue & T. Tanaka, (1986) The M1- and M2-type isozymes of rat pyruvate kinase are produced from the same gene by alternative RNA splicing. *J Biol Chem* **261**: 13807-13812.

Nosworthy, N.J., A. Peterkofsky, S. Konig, Y.J. Seok, R.H. Szczepanowski & A. Ginsburg, (1998) Phosphorylation destabilizes the amino-terminal domain of enzyme I of the *Escherichia coli* phosphoenolpyruvate:sugar phosphotransferase system. *Biochemistry* **37**: 6718-6726.

Nowakowska, J. & J.D. Oliver, (2013) Resistance to environmental stresses by *Vibrio vulnificus* in the viable but nonculturable state. *FEMS Microbiol Ecol* **84**: 213-222.

Oliver, J.D., (2010) Recent findings on the viable but nonculturable state in pathogenic bacteria. *FEMS Microbiol Rev* **34**: 415-425.

Oliver, J.D. & R. Bockian, (1995) In vivo resuscitation, and virulence towards mice, of viable but nonculturable cells of *Vibrio vulnificus*. *Appl Environ Microbiol* **61**: 2620-2623.

Oliver, J.D., F. Hite, D. Mcdougald, N.L. Andon & L.M. Simpson, (1995) Entry into, and resuscitation from, the viable but nonculturable state by *Vibrio vulnificus* in an estuarine environment. *Appl Environ Microbiol* **61**: 2624-2630.

Otto, B.R., A.M. Verweij-van Vught & D.M. MacLaren, (1992) Transferrins and heme-compounds as iron sources for pathogenic bacteria. *Crit Rev Microbiol* **18**: 217-233.

Park, Y.H., B.R. Lee, Y.J. Seok & A. Peterkofsky, (2006) *In vitro* reconstitution of catabolite repression in *Escherichia coli*. *J Biol Chem* **281**: 6448-6454.

Park, Y.H., C.R. Lee, M. Choe & Y.J. Seok, (2013) HPr antagonizes the anti-sigma70 activity of Rsd in *Escherichia coli*. *Proc Natl Acad Sci U S A* **110**: 21142-21147.

Peterkofsky, A., A. Reizer, J. Reizer, N. Gollop, P.P. Zhu & N. Amin, (1993) Bacterial adenylyl cyclases. *Prog Nucleic Acid Res Mol Biol* **44**: 31-65.

Ponce, E., N. Flores, A. Martinez, F. Valle & F. Bolivar, (1995) Cloning of the two pyruvate kinase isoenzyme structural genes from *Escherichia coli*: the relative roles of these enzymes in pyruvate biosynthesis. *J Bacteriol* **177**: 5719-5722.

Ponce, E., A. Martinez, F. Bolivar & F. Valle, (1998) Stimulation of glucose catabolism through the pentose pathway by the absence of the two pyruvate kinase isoenzymes in *Escherichia coli*. *Biotechnol Bioeng* **58**: 292-295.

Postma, P.W., J.W. Lengeler & G.R. Jacobson, (1993) Phosphoenolpyruvate:carbohydrate phosphotransferase systems of bacteria. *Microbiol Rev* **57**: 543-594.

Powell, B.S., D.L. Court, T. Inada, Y. Nakamura, V. Michotey, X. Cui, A. Reizer, M.H. Saier, Jr. & J. Reizer, (1995) Novel proteins of the phosphotransferase system encoded within the *rpoN* operon of *Escherichia coli*. Enzyme IIA^{Ntr} affects growth on organic nitrogen and the conditional lethality of an erats mutant. *J Biol Chem* **270**: 4822-4839.

Presper, K.A., C.Y. Wong, L. Liu, N.D. Meadow & S. Roseman, (1989) Site-directed mutagenesis of the phosphocarrier protein. III^{Glc}, a major signal-transducing protein in *Escherichia coli*. *Proc Natl Acad Sci U S A* **86**: 4052-4055.

Rigden, D.J., S.E. Phillips, P.A. Michels & L.A. Fothergill-Gilmore, (1999) The structure of pyruvate kinase from *Leishmania mexicana* reveals details of the allosteric transition and unusual effector specificity. *J Mol Biol* **291**: 615-635.

Robillard, G.T. & J. Broos, (1999) Structure/function studies on the bacterial carbohydrate transporters, enzymes II, of the phosphoenolpyruvate-dependent phosphotransferase system. *Biochim Biophys Acta* **1422**: 73-104.

Rohwer, J.M., N.D. Meadow, S. Roseman, H.V. Westerhoff & P.W. Postma, (2000) Understanding glucose transport by the bacterial phosphoenolpyruvate:glycose phosphotransferase system on the basis of kinetic measurements *in vitro*. *J Biol Chem* **275**: 34909-34921.

Sakai, H., K. Suzuki & K. Imahori, (1986) Purification and properties of pyruvate kinase from *Bacillus stearothermophilus*. *J Biochem* **99**: 1157-1167.

Sassetti, C.M., D.H. Boyd & E.J. Rubin, (2003) Genes required for mycobacterial growth defined by high density mutagenesis. *Mol Microbiol* **48**: 77-84.

Seok, Y.J., B.M. Koo, M. Sondej & A. Peterkofsky, (2001) Regulation of *E. coli* glycogen phosphorylase activity by HPr. *J Mol Microbiol Biotechnol* **3**: 385-393.

Seok, Y.J., B.R. Lee, P.P. Zhu & A. Peterkofsky, (1996) Importance of the carboxyl-terminal domain of enzyme I of the *Escherichia coli* phosphoenolpyruvate: sugar phosphotransferase system for phosphoryl donor specificity. *Proc Natl Acad Sci U S A* **93**: 347-351.

Seok, Y.J., M. Sondej, P. Badawi, M.S. Lewis, M.C. Briggs, H. Jaffe & A. Peterkofsky, (1997a) High affinity binding and allosteric

regulation of *Escherichia coli* glycogen phosphorylase by the histidine phosphocarrier protein, HPr. *J Biol Chem* **272**: 26511-26521.

Seok, Y.J., J. Sun, H.R. Kaback & A. Peterkofsky, (1997b) Topology of allosteric regulation of lactose permease. *Proc Natl Acad Sci U S A* **94**: 13515-13519.

Seok, Y.J., P.P. Zhu, B.M. Koo & A. Peterkofsky, (1998) Autophosphorylation of enzyme I of the *Escherichia coli* phosphoenolpyruvate:sugar phosphotransferase system requires dimerization. *Biochem Biophys Res Commun* **250**: 381-384.

Shapiro, R.L., S. Altekruse, L. Hutwagner, R. Bishop, R. Hammond, S. Wilson, B. Ray, S. Thompson, R.V. Tauxe & P.M. Griffin, (1998) The role of Gulf Coast oysters harvested in warmer months in *Vibrio vulnificus* infections in the United States, 1988-1996. . *J Infect Dis* **178**: 752-759.

Shelburne, S.A., 3rd, D. Keith, N. Horstmann, P. Sumby, M.T. Davenport, E.A. Graviss, R.G. Brennan & J.M. Musser, (2008) A direct link between carbohydrate utilization and virulence in the major human pathogen group A *Streptococcus*. *Proc Natl Acad Sci U S A* **105**: 1698-1703.

Siebold, C., K. Flukiger, R. Beutler & B. Erni, (2001) Carbohydrate transporters of the bacterial phosphoenolpyruvate: sugar phosphotransferase system (PTS). *FEBS Lett* **504**: 104-111.

Signoretto, C., M.M. Lleo, M.C. Tafi & P. Canepari, (2000) Cell wall chemical composition of *Enterococcus faecalis* in the viable but nonculturable state. *Appl Environ Microbiol* **66**: 1953-1959.

Simon, R., U. Priefer & A. Puhler, (1983) A broad host range mobilization system for *In vivo* genetic engineering: transposon mutagenesis in gram-negative bacteria. *Bio-Technology* **1**: 784-791.

Song, J.H., K.S. Ko, J.Y. Lee, J.Y. Baek, W.S. Oh, H.S. Yoon, J.Y. Jeong & J. Chun, (2005) Identification of essential genes in *Streptococcus pneumoniae* by allelic replacement mutagenesis. *Mol Cells* **19**: 365-374.

Speranza, M.L., G. Valentini, P. Iadarola, M. Stoppini, M. Malcovati & G. Ferri, (1989) Primary structure of three peptides at the catalytic and allosteric sites of the fructose-1,6-bisphosphate-activated pyruvate-kinase from *Escherichia-Coli*. *Biol Chem Hoppe-Seyler* **370**: 211-216.

Strom, M.S. & S. Lory, (1993) Structure-function and biogenesis of the type IV pili. *Annu Rev Microbiol* **47**: 565-596.

Strom, M.S. & R.N. Paranjpye, (2000) Epidemiology and pathogenesis of *Vibrio vulnificus*. *Microbes Infect* **2**: 177-188.

Stuart, D.I., M. Levine, H. Muirhead & D.K. Stammers, (1979) Crystal structure of cat muscle pyruvate kinase at a resolution of 2.6 A. *J Mol Biol* **134**: 109-142.

Stulke, J. & W. Hillen, (1999) Carbon catabolite repression in bacteria. *Curr Opin Microbiol* **2**: 195-201.

Suzuki, K., S. Ito, A. Shimizu-Ibuka & H. Sakai, (2008) Crystal structure of pyruvate kinase from *Geobacillus stearothermophilus*. *J Biochem* **144**: 305-312.

Tacket, C.O., F. Brenner & P.A. Blake, (1984) Clinical features and an epidemiological study of *Vibrio vulnificus* infections. *J Infect Dis* **149**: 558-561.

Takahashi, H., T. Inada, P. Postma & H. Aiba, (1998) CRP down-regulates adenylate cyclase activity by reducing the level of phosphorylated IIA^{Glc}, the glucose-specific phosphotransferase protein, in *Escherichia coli*. *Mol Gen Genet* **259**: 317-326.

Tanaka, Y., K. Kimata & H. Aiba, (2000) A novel regulatory role of glucose transporter of *Escherichia coli*: membrane sequestration of a global repressor Mlc. *EMBO J* **19**: 5344-5352.

Thomson, C.J., E. Power, H. Ruebsamen-Waigmann & H. Labischinski, (2004) Antibacterial research and development in the 21(st) Century--an industry perspective of the challenges. *Curr Opin Microbiol* **7**: 445-450.

Troxell, B., J.J. Zhang, T.J. Bourret, M.Y. Zeng, J. Blum, F. Gherardini, H.M. Hassan & X.F. Yang, (2014) Pyruvate protects pathogenic spirochetes from H_2O_2 killing. *PLoS One* **9**: e84625.

Tsvetanova, B., A.C. Wilson, C. Bongiorni, C. Chiang, J.A. Hoch & M. Perego, (2007) Opposing effects of histidine phosphorylation regulate the AtxA virulence transcription factor in *Bacillus anthracis*. *Mol Microbiol* **63**: 644-655.

Ugurbil, K., H. Rottenberg, P. Glynn & R.G. Shulman, (1982) Phosphorus-31 nuclear magnetic resonance studies of bioenergetics in wild-type and adenosinetriphosphatase(1-) *Escherichia coli* cells. *Biochemistry* **21**: 1068-1075.

Valentini, G., L. Chiarelli, R. Fortin, M.L. Speranza, A. Galizzi & A. Mattevi, (2000) The allosteric regulation of pyruvate kinase. *J Biol Chem* **275**: 18145-18152.

Valentini, G., L.R. Chiarelli, R. Fortin, M. Dolzan, A. Galizzi, D.J. Abraham, C. Wang, P. Bianchi, A. Zanella & A. Mattevi, (2002) Structure and function of human erythrocyte pyruvate kinase.

Molecular basis of nonspherocytic hemolytic anemia. *J Biol Chem* **277**: 23807-23814.

van Schaftingen, E., F.R. Opperdoes & H.G. Hers, (1985) Stimulation of *Trypanosoma brucei* pyruvate kinase by fructose 2,6-bisphosphate. *Eur J Biochem* **153**: 403-406.

Waygood, E.B., J.S. Mort & B.D. Sanwal, (1976) The control of pyruvate kinase of *Escherichia coli*. Binding of substrate and allosteric effectors to the enzyme activated by fructose 1,6-bisphosphate. *Biochemistry* **15**: 277-282.

Waygood, E.B. & B.D. Sanwal, (1974) The control of pyruvate kinases of *Escherichia coli*. I. Physicochemical and regulatory properties of the enzyme activated by fructose 1,6-diphosphate. *J Biol Chem* **249**: 265-274.

Whitesides, M.D. & J.D. Oliver, (1997) Resuscitation of *Vibrio vulnificus* from the viable but nonculturable state. *Appl Environ Microbiol* **63**: 1002-1005.

Wright, A.C. & J.G. Morris, Jr., (1991) The extracellular cytolysin of *Vibrio vulnificus*: inactivation and relationship to virulence in mice. *Infect Immun* **59**: 192-197.

Wright, A.C., L.M. Simpson, J.D. Oliver & J.G. Morris, Jr., (1990) Phenotypic evaluation of acapsular transposon mutants of *Vibrio vulnificus*. *Infect Immun* **58**: 1769-1773.

Xavier, K.B., M. Kossmann, H. Santos & W. Boos, (1995) Kinetic analysis by in vivo ^{31}P nuclear magnetic resonance of internal P_i during the uptake of *sn*-glycerol-3-phosphate by the *pho* regulon-dependent Ugp system and the *glp* regulon-dependent GlpT system. *J Bacteriol* **177**: 699-704.

Xu, H.S., N. Roberts, F.L. Singleton, R.W. Attwell, D.J. Grimes & R.R. Colwell, (1982) Survival and viability of nonculturable *Escherichia coli* and *Vibrio cholerae* in the estuarine and marine environment. *Microb Ecol* **8**: 313-323.

Yamamoto, K., A.C. Wright, J.B. Kaper & J.G. Morris, Jr., (1990) The cytolysin gene of *Vibrio vulnificus*: sequence and relationship to the *Vibrio cholerae* E1 Tor hemolysin gene. *Infect Immun* **58**: 2706-2709.

Zhang, R., H.Y. Ou & C.T. Zhang, (2004) DEG: a database of essential genes. *Nucleic Acids Res* **32**: D271-272.

Zoraghi, R., R.H. See, H. Gong, T. Lian, R. Swayze, B.B. Finlay, R.C. Brunham, W.R. McMaster & N.E. Reiner, (2010) Functional analysis, overexpression, and kinetic characterization of

pyruvate kinase from methicillin-resistant *Staphylococcus aureus*. *Biochemistry* **49**: 7733-7747.

Zoraghi, R., L. Worrall, R.H. See, W. Strangman, W.L. Popplewell, H. Gong, T. Samaai, R.D. Swayze, S. Kaur, M. Vuckovic, B.B. Finlay, R.C. Brunham, W.R. McMaster, M.T. Davies-Coleman, N.C. Strynadka, R.J. Andersen & N.E. Reiner, (2011) Methicillin-resistant *Staphylococcus aureus* (MRSA) pyruvate kinase as a target for bis-indole alkaloids with antibacterial activities. *J Biol Chem* **286**: 44716-44725.

국문초록

세균의 phosphoenolpyruvate:sugar phosphotransferase system (PTS) 은 모든 당에 공통된 단백질인 Enzyme I (EI) 과 HPr, 그리고 당에 특이적인 Enzyme II (EII) 단백질들 사이의 인산기 전달을 통해 여러 가지 당의 수송을 매개할 수 있다. 대표적인 예로 포도당 특이적인 PTS 의 EII 는 세포질에 위치한 단백질인 enzyme IIA^{Glc} ($EIIA^{Glc}$) 와 세포막에 위치한 enzyme $IICB^{Glc}$ ($EIICB^{Glc}$) 로 구성되어 있다. 이 PTS 는 외부에 포도당이 존재할 때, 세포내의 PEP 로부터 EI → HPr → $EIIA^{Glc}$ → $EIICB^{Glc}$ 순으로 인산기를 전달하고 최종적으로는 세포 내로 들어온 포도당에 인산기를 전달하여 당을 수송한다. PTS 의 구성 단백질들은 당의 수송을 매개할 뿐만 아니라 세포내의 생리 활성 조절과 관련된 다양한 역할들을 수행한다고도 알려져 있다. 예를 들어, 대장균의 $EIIA^{Glc}$ 는 인산화 상태에 따라 adenylate cyclase, fermentation/respiration switch protein, glycerol kinase 의 활성 조절, inducer exclusion 과 같은 여러 가지 역할을 수행한다. 대장균에서 PTS 구성 단백질들의 기능이 심도 깊게 연구되고 있는데 반해 패혈증 비브리오균에서 PTS 의 생리적인 역할은 거의

밝혀져 있지 않다. 패혈증 비브리오균 (*Vibrio vulnificus*) 은 그람 음성 간균이며, 하나의 편모로 운동성을 갖는 해양 세균이다. 특히 이 균은 기회 감염균으로 이 균으로 오염된 해산물을 날 것으로 섭취하거나, 몸의 상처를 통해 이 균이 감염될 경우 심각한 패혈증이 유발될 수 있다. 당뇨병 환자나 간이 손상된 사람, 면역력이 약화된 사람들의 경우 이 균에 감염되면 패혈증으로 사망할 확률이 50% 이상으로 정상인보다 상당히 높다.

패혈증 비브리오균에서 PTS 의 생리적인 조절 작용을 알아보기 위해 PTS 구성 단백질인 HPr 과 상호작용하는 단백질을 찾기로 하고, HPr 을 bait 으로 하여 ligand fishing 실험을 수행하였다. 그 결과 패혈증 비브리오균에 존재하는, HPr 과 상호작용하는 단백질은 대장균의 pyruvate kinase A (ePykA) 와 유사한 염기서열을 갖는 효소였고, 이것의 이름을 따서 비브리오의 pyruvate kinase A (vPykA) 라고 명명하였다. Pyruvate kinase (PK) 는 해당과정의 마지막 단계에 작용하는 효소로 PEP 의 인산기를 ADP 로 전달하여 ATP 와 pyruvate 를 생성하는 반응을 촉매한다. 특이하게도 패혈증 비브리오균의 HPr 과 vPykA 의 상호작용은 inorganic phosphate 의 농도에 비례하여 이루어졌다. 또한 탈인산화된 HPr 만이 vPykA 와 상호작용할 수 있었다. 이러한 상호작용은 대장균에서는 일어나지 않았으며, 비브리오균에서의 종 특이적인

상호작용임을 알 수 있었다. 대장균과 비브리오균의 PykA 들 간의 domain swapping 실험을 통해, vPykA 가 비브리오균의 HPr 과 상호작용할 때 vPykA 의 C-terminal domain 이 반드시 필요하다는 것을 확인하였다. PK 의 C-terminal domain 은 allosteric effector 들이 작용하는 부분이라고 알려져 있었기 때문에 우리는 HPr 이 vPykA 의 allosteric regulator 로 작용할 수 있는지 확인해 보기로 하였다. vPykA 의 활성은 lactate dehydrogenase (LDH)-coupled enzyme assay 를 통해 측정하였고, 이 반응에서 vPykA 의 활성이 좋을수록 빠르게 ATP 와 pyruvate 가 생성되고 연이어 LDH 에 의해 NADH 가 빠르게 산화되는 것을 관찰할 수 있었다. 특히 vPykA 는 인산화된 HPr 이 있을 때 보다 탈인산화된 HPr 이 있을 때 PEP 에 대한 K_m 값이 약 4 배 가량 감소되는 현상을 보였다.

vPykA 의 생리적인 역할을 밝히기 위해 inframe deletion 으로 *vpykA* 결손 균주를 제작하였다. *vpykA* 결손 균주는 야생형 균주와 동일한 수의 균들을 4 ℃ 에 보관했을 때 빠르게 viable but nonculturable (VBNC) 상태가 되었다. VBNC 상태는 여러 그람 음성균에서 나타나는 현상으로 낮은 온도 또는 스트레스 상황에서 세균이 살아는 있지만 실험실 배지에서는 키울 수 없게 되는

현상이다. 추운 겨울 바다에서 VBNC 상태를 보이는 패혈증 비브리오균에서도 활발하게 연구가 이루어지고 있다. 다수의 연구들에서 catalase 나 pyruvate 같은 H_2O_2 scavenger 가 첨가된 배지에서는 VBNC 상태가 호전되는 것을 통해 VBNC 상태와 reactive oxygen species (ROS)의 연관성을 증명하였다. 흥미롭게도 *vpykA* 결손 균주는 야생형 균주보다 H_2O_2 에 더 민감하였고, 이런 민감성은 배지에 pyruvate 를 첨가해 줄 경우 회복되었다. 이런 결과들을 바탕으로 외부에 포도당이 존재할 때 비브리오균의 HPr 이 탈인산화되면서 vPykA 를 활성화 시키고 결과적으로 H_2O_2 에 더 강한 저항성을 갖게 된다는 것을 알 수 있었다.

주요어 : H_2O_2 stress, 인산전달계, 단백질-단백질 상호작용, 해당과정 조절, 패혈증 비브리오균

학번: 2010-30095